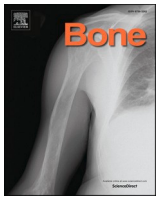
Bone 195 (2025) 117472



Contents lists available at ScienceDirect

Bone

journal homepage: www.elsevier.com/locate/bone



Full Length Article

The GWAS candidate far upstream element binding protein 3 (FUBP3) is required for normal skeletal growth, and adult bone mass and strength in mice

Laura M. Watts, Penny C. Sparkes, Hannah F. Dewhurst, Siobhan E. Guilfoyle, Andrea S. Pollard, Davide Komla-Ebri, Natalie C. Butterfield, Graham R. Williams *, J.H. Duncan Bassett *

Molecular Endocrinology Laboratory, Department of Metabolism, Digestion and Reproduction, Imperial College London, London, UK

ARTICLE INFO

Keywords:
FUBP3
Osteoporosis
Genome wide association study
Knockout mouse

ABSTRACT

Bone mineral density (BMD) and height are highly heritable traits for which hundreds of genetic loci have been linked through genome wide association studies (GWAS). FUBP3 is a DNA and RNA binding protein best characterised as a transcriptional regulator of *c-Myc*, but little is known about its role *in vivo*. Single nucleotide polymorphisms in *FUBP3* at the 9q34.11 locus have been associated with BMD, fracture and height in multiple GWAS, but FUBP3 has no previously established role in the skeleton. We analysed *Fubp3*-deficient mice to determine the consequence of FUBP3 deficiency *in vivo*. Mice lacking *Fubp3* had reduced survival to adulthood and impaired skeletal growth. Bone mass was decreased, most strikingly in the vertebrae, with altered trabecular micro-architecture. *Fubp3* deficient bones were also weak. These data provide the first functional demonstration that *Fubp3* is required for normal skeletal growth and development and maintenance of adult bone structure and strength, indicating that *FUBP3* contributes to the GWAS association of 9q34.11 with variation in height, BMD and fracture.

1. Introduction

Bone mineral density (BMD) and height are highly heritable traits [1–3]. Decreased BMD is a diagnostic criterion for osteoporosis [4] and a major risk factor for fracture with its associated burden of morbidity and mortality [5–8], whilst final adult height reflects skeletal growth during development. Genome Wide Association Studies (GWAS) have identified hundreds of loci associated with BMD and height, including multiple single nucleotide polymorphisms (SNPs) in and around the *FUBP3* gene [9–20]. However, little is known regarding the role of *FUBP3 in vivo* and it has no well characterised role in skeletal physiology. As for many GWAS loci, the *FUBP3* associations lie in non-coding regions and functional validation is required to determine the genetic basis of the association signal and its relevance to the skeleton [21–24]. We investigated *Fubp3* knockout mice to study the role of *Fubp3* in the skeleton and determine whether it is a likely candidate underlying the 9q34.11 association with variation in BMD, fracture and height.

FUBP3 is the third member of a family of single stranded-DNA and RNA binding proteins best characterised as regulators of the proto-oncogene *c-Myc* through its Far Upstream Sequence Element (FUSE) [25,26]. SNPs in the *FUBP3* gene at the 9q34.11 locus have been robustly associated with BMD, fracture and height in multiple GWAS [9–20]. Whilst FUBP1 has essential roles in embryonic development and may be involved in oncogenesis [27–30], and FUBP2 is characterised as a regulator of mRNA processing and stability [31,32] with broad functions including immune homeostasis [33], development [34] and tumourigenesis [35], much less is known about the normal function of FUBP3 *in vivo*.

Additional evidence provides the rationale for further investigation of *FUBP3* as a likely causative gene underlying the 9q34.11 association with BMD, fracture and height. In addition to the GWAS lead SNPs lying within introns of the *FUBP3* gene itself [9,10], C-MYC has roles in bone physiology including skeletal development and age-related bone turnover [36–38]. *FUBP3* is expressed across a broad range of tissues [39] (https://www.gtexportal.org/home/gene/FUBP3, accessed 7/11/2024) but in the skeleton, expression has been documented in osteoblasts and

* Corresponding authors at: Molecular Endocrinology Laboratory, The Commonwealth Building, Hammersmith Hospital, Du Cane Road, London W12 0NN, UK.
E-mail addresses: graham.williams@imperial.ac.uk (G.R. Williams), d.bassett@imperial.ac.uk (J.H.D. Bassett).

https://doi.org/10.1016/j.bone.2025.117472
Received 31 December 2024; Received in revised form 14 March 2025; Accepted 23 March 2025
Available online 24 March 2025
8756-3282/© 2025 The Authors. Published by Elsevier Inc. This is an open access article under the CC BY license (http://creativecommons.org/licenses/by/4.0/).

osteoclasts [15]. Furthermore, FUBP3 may regulate translation of FGF9, which has key functions in skeletal development and bone repair, and is a causative gene for the multiple synostosis syndrome [40–44]. Nevertheless, FUBP3 itself has no established role in the skeleton and GWAS follow up approaches are limited by a lack of functional knowledge regarding the non-coding genome, inability to separate associated variants due to patterns of linkage disequilibrium, and a paucity of bone specific data in bioinformatics databases [23]. The mouse has been extensively used as a model for understanding the skeletal function of genes and specifically for functional validation of GWAS candidate genes [14,15,45]. This *in vivo* approach allows the characterisation of the effects of a genetic alteration in a complex system comprising interacting endocrine, paracrine and biomechanical factors [14,15].

We proposed that *FUBP3* contributes to the GWAS association with height, BMD and fracture at the 9q34.11 locus. To investigate this hypothesis, we characterised the skeletal consequences of *Fubp3*-defieiency in knockout mice and demonstrated that *Fubp3* is required for normal linear growth, bone mineralisation and strength in mice.

2. Materials and methods

2.1. GWAS prioritisation

GWAS reporting an association between *FUBP3* variants and BMD or fracture were identified by searching the NHGRI-EBI-GWAS catalogue (www.ebi.ac.uk/gwas) and data were combined to generate regional association plots in LocusZoom (locuszoom.org, [46]). Linkage disequilibrium and haplotype relationships between *FUBP3* GWAS SNPs were interrogated in the LDLink suite of tools (ldlink.nci.nih.gov).

2.2. Animal methods

Fubp3$^{+/-}$ mice were generated by *in vitro* fertilisation using sperm from mice heterozygous for the *Fubp3*$^{tm1a(KOMP)Wtsi}$ allele (Wellcome Trust Sanger Institute, Hinxton, UK, [47]) and oocytes from C57BL/6N mice. The knockout allele used was generated as part of the International Knockout Mouse Programme using their standard methodology [47]. Details of the *Fubp3*$^{tm1a(KOMP)Wtsi}$ allele are provided in Supplementary methods and Supplementary Fig. 1. *Fubp3*$^{+/-}$ mice were bred to produce *Fubp3*$^{+/+}$, *Fubp3*$^{+/-}$ and *Fubp3*$^{-/-}$ mice. All animals were housed in individually ventilated cages with *ad libitum* access to food and water and 12-h light/dark cycles. All experiments were conducted in accordance with the Animals (Scientific Procedures) Act 1986 under appropriate project and personal licences and additionally approved by the Animal Welfare and Ethical Review Body at Imperial College London.

Mice were weaned at 21 days of age and genotyped by polymerase chain reaction (PCR) of genomic DNA from ear clip samples (Supplementary methods, Supplementary fig. 1). Mice were euthanised at postnatal days P1, P21, P70 and P183 according to approved Schedule 1 procedures with appropriate confirmation, soft tissue was removed and the skeleton dissected for either storage in 70 % ethanol, or fixation in 10 % neutral buffered formalin (NBF) and storage in 70 % ethanol. Mice received intravenous injections of 2.5 mg/kg fluorescent calcein (0.5 mg/ml, Sigma-Aldrich, UK) at 1 and 4/5 days prior to euthanasia at P70 and P183. Blood for serum sampling was obtained by cardiac puncture immediately prior to sacrifice at P70 and P183, allowed to clot, spun at 5000G for 15 min and supernatant removed and stored at −80 °C until use. Ovariectomy was performed at P70 under isoflurane anaesthesia according to established protocols [48]. Lumbar vertebral specimens were collected and analysed 6 weeks later (P112).

2.3. Radiological imaging

Bone mineral content (BMC) was determined in left hindlimbs, proximal tail vertebrae and lumbar vertebrae 5–6 using a Faxitron Ultrafocus (Faxitron Bioptics, Tucson, Arizona, USA) and VisionDXA software operating at 22 kV for 20 s, with steel, plastic and aluminium standards as previously described [49,50].

Trabecular and cortical bone parameters were determined on micro-CT images of femurs and lumbar vertebrae at P70 and P183 using a Scanco μCT 50 (Scanco Medical, Switzerland) operating at 70 kV, 1 s integration time, 500 projections per 180° and with 0.5 mm aluminium filter. All samples were imaged in 70 % ethanol. Analysis was performed using the Scanco μCT Evaluation Programme (v6.6). Femur cortical parameters (cortical thickness, internal cortical diameter, cortical BMD, total cortical cross-sectional area, cortical bone area, cortical area/total area) were determined on a 1.5 mm region of interest (ROI) 56 % of the distance from the proximal to the distal femur scanned at 10 μm voxel resolution. High resolution (1 μm voxel resolution) scans were performed on a 0.5 mm region 56 % of the distance from the proximal to the distal femur at P70 to determine cortical porosity and canal diameter. Trabecular parameters (trabecular number, trabecular thickness, trabecular separation, bone volume/tissue volume and trabecular BMD) were determined for femurs and lumbar vertebrae scanned at 5 μm voxel resolution. Contours were applied defining the trabecular compartment and excluding cortical bone [51]. Femoral analysis was performed on a 1 mm ROI commencing 100 μm proximal to the distal femoral growth plate. Lumbar analysis included the whole vertebral trabecular compartment.

2.4. P1 imaging

P1 mice were eviscerated and the skin removed, fixed in 95 % ethanol, placed in acetone for fat removal, and stained in 0.015 % alcian blue and 0.005 % alizarin red followed by destaining in 1 % potassium hydroxide with increasing proportions of glycerol (0, 20, 40, 60 80 %) for 72 h each. Samples were stored in 100 % glycerol, imaged using an HP Scanjet G2710 flatbed photo scanner with standard of known length, and limb and nose-to-tail lengths were measured blinded to genotype using ImageJ 1.44.

2.5. Growth plate histology

Hindlimbs from P21 mice fixed in 10 % NBF were decalcified in 12.5 % EDTA, pH 7.4 for 14 days with one EDTA change. Paraffin embedded mid-tibial sagittal sections were stained with Alcian blue and van Gieson, images were acquired using a Leica DM LB2 microscope and Flexacam C1 camera assembled to give a complete image, and measurements were taken at five locations across the growth plate width using ImageJ as previously described [52,53]. Two midline sections were examined per specimen.

2.6. Confocal microscopy for analysis of bone formation

L1 lumbar vertebrae fixed in 10 % NBF were embedded in polymethyl methacrylate (PMMA) and polished to an optically flat finish in the mid-coronal plane [52,53]. Calcein labels were examined by confocal laser scanning microscopy (CSLM) [52,53] using a Leica SP5 confocal microscope at 488 nm excitation and 40× objective. Montages of overlapping CSLM fields covering the whole inner trabecular region of the L1 vertebra, excluding cortical surfaces, were used for analysis. Mineralising surface (MS) was calculated from measurement of the lengths of single and double calcein labelled surfaces and the bone surface. Separation between calcein double labels was calculated perpendicular to label surface at five points along each double label length. Two dimensional bone formation parameters were calculated according to the guidelines from the American Society of Bone and Mineral Research [54].

2.7. Osteoclast histomorphometry

Two paraffin embedded proximal tibial mid-line sections from the hindlimbs of P70 mice fixed in 10 % NBF and decalcified in 12.5 % EDTA were stained for TRAP activity. Two proximal tibial mid-line sections were imaged per sample using a Leica DM LB2 microscope with Flexacam C1 at 10× magnification and overlapping images were assembled. Analysis was performed on a 750 μm × 750 μm ROI placed 100 μm below the distal edge of the proximal tibial growth plate using TrapHisto software as per instructions [55] to determine osteoclasts in contact with the bone surface.

2.8. Biomechanical testing

Biomechanical testing was performed using an Instron 5543 load frame (Instron, UK) as previously described [52,53]. Femurs were placed horizontally centred on rounded support pins with a span of 8 mm and load was applied perpendicular to the midshaft of the femur using a 100 N load cell and a constant rate of displacement of 0.03 mm/s until fracture [53]. L6 lumbar vertebrae were prepared for compression testing by carefully removing vertebral processes using a cylindrical dental burr to isolate the vertebral body, confirmed by Faxitron X-ray microradiographical imaging. Vertebrae were attached to the load cell platform in a proximal-distal orientation using glue. Vertical alignment was confirmed, and vertebrae were compressed along their proximo-distal axis using the load frame fitted with 500 N load cell at a rate of displacement of 0.03 mm/s until approximately 0.5 mm of displacement. Yield load, maximum load, stiffness and for femurs, fracture load were determined from load-displacement curves.

2.9. Statistical methods

Statistical analysis was performed in GraphPad Prism 9, other than for x-ray microradiography for which Microsoft Excel was used. Data were analysed using Chi-squared test, Student's *t*-test or one way analysis of variance (ANOVA) with post-hoc Tukey test as indicated. Frequency distributions of grey level intensities obtained by Faxitron x-ray microradiography were compared using the Kolmogorov-Smirnov test [50,52]. *P* values of <0.05 were considered significant. Based upon previous work in our laboratory, a minimum sample size of 6 mice per group was calculated as being needed to detect a 20 % difference at 90 % power for the imaging analysis method with the largest variation (histomorphometry). Lumbar vertebral compression testing demonstrates greater variability, and a minimum sample size of 14 mice per group is needed to detect a 20 % difference in lumbar yield load at 90 % power.

3. Results

3.1. Prioritisation of FUBP3 from the 9q34.11 GWAS locus for functional validation

Combining publicly available GWAS BMD association data and analysis of lead SNPs for linkage disequilibrium demonstrates that the 9q34.11 association with BMD and fracture is formed by a tight cluster of co-inherited SNPs in and immediately around the *FUBP3* gene forming a risk haplotype (Supplementary Fig. 2, Supplementary Table 1). Two genes in the 1 Mb regions surrounding *FUBP3* are associated with human childhood developmental abnormalities, *EXOSC2* with a syndrome including short stature, and gain of function variants in *ABL1* with a syndrome of cardiac abnormalities, scoliosis, hindfoot deformity and finger contractures (Supplementary table 2). In both, the GWAS association falls away before these genes and reduced BMD and fractures are not known to be features of these conditions.

3.2. Fubp3 deficiency affects postnatal development and growth

Fubp3$^{-/-}$ mice reproduced normally, were viable, and survived to adulthood. However, significantly fewer *Fubp3*$^{-/-}$ mice were present at weaning than the expected Mendelian ratio (20 % *vs* the expected 25 % from two *Fubp3*$^{+/-}$ parents, $P = 0.007$, Chi-squared test, Supplementary fig. 3). There was no significant difference in average litter size between *Fubp3*$^{+/+}$, *Fubp3*$^{+/-}$ and *Fubp3*$^{-/-}$ parents (Supplementary fig. 3) and the average interval between litters did not differ between genotypes (data not shown).

No effect of *Fubp3* deficiency on early skeletal development (Fig. 1, minimum 5 per genotype examined) was seen on examination of alizarin red and alcian blue stained P1 mouse skeletons. However, *Fubp3*$^{-/-}$ mice demonstrated impaired postnatal growth compared to *Fubp3*$^{+/+}$ animals (Fig. 1). *Fubp3*$^{-/-}$ mice demonstrated 3–5 % reductions in nose-tail length at P70 (female $P = 0.005$, male $P = 0.051$) and P183 (female $P = 0.009$, male $P < 0.0001$) and 3–7 % reductions in tail length at P70 (female $P < 0.0001$, male $P = 0.001$) and P183 (female $P = 0.002$, male $P = 0.004$) compared to *Fubp3*$^{+/+}$ animals (one-way ANOVA, Supplementary fig. 4). Consistent with this, *Fubp3*$^{-/-}$ mice had significantly shorter tibiae (P70: female $P = 0.004$, male $P = 0.004$; P183 female $P = 0.0003$, male $P = 0.0002$, *t*-test) and caudal vertebrae (P70: female $P = 0.0009$, male $P = 0.18$; P183 female and male $P < 0.0001$, one way ANOVA with post-hoc Tukey test) than their wild type counterparts (Supplementary fig. 5). There was no significant effect of *Fubp3* deficiency on femur length.

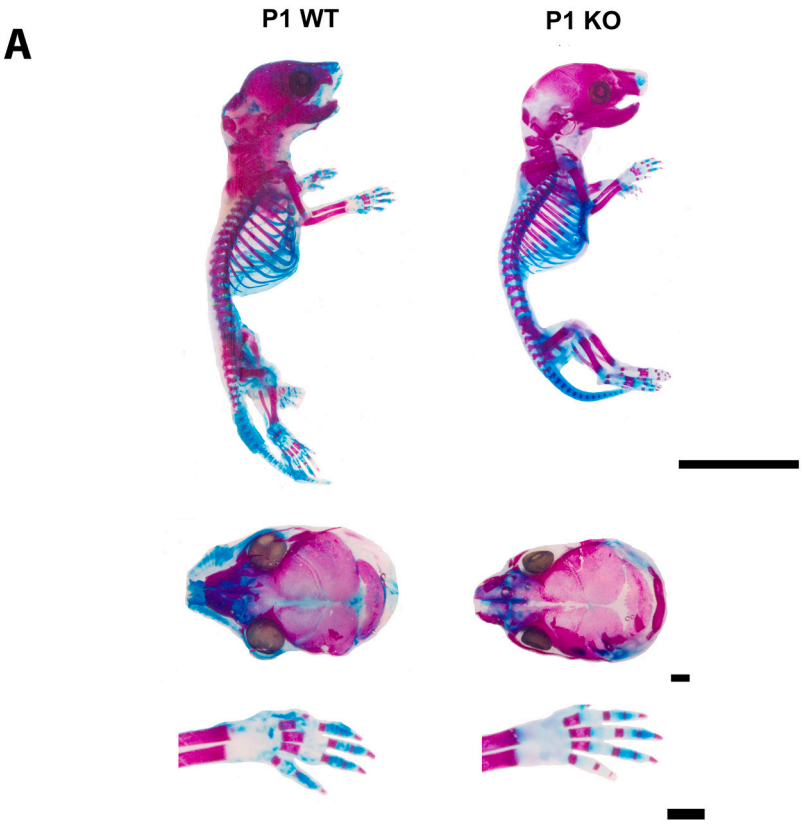
Histological examination of the tibial growth plate at P21 demonstrated that *Fubp3*$^{-/-}$ mice had significantly smaller overall growth plate width compared to *Fubp3*$^{+/+}$ mice ($P = 0.004$, *t*-test) due to decreased total width of the hypertrophic ($P < 0.0004$) and proliferative zones ($P = 0.003$, two-way ANOVA with Sidak multiple comparison test). Nevertheless, growth plate zones remained in proportion with no evidence of growth plate disorganisation or abnormal chondrocyte differentiation (Fig. 1).

3.3. Fubp3 deficiency results in decreased bone mineral content and abnormal trabecular bone parameters

Male and female *Fubp3*$^{-/-}$ mice displayed a markedly decreased bone mineral content of L5 and L6 vertebrae at P70 and P183 (Fig. 2A, Supplementary fig. 6, $P < 0.001$, Kolmogorov-Smirnov test). Consistent with this, micro-CT of L1 vertebrae demonstrated reduced trabecular thickness (P70: male $P = 0.005$, female $P = 0.017$; P183 male $P = 0.0096$, female $P = 0.005$), and decreased trabecular bone mineral density (P70: male $P = 0.002$, female $P = 0.002$; P183 male $P = 0.015$) (Fig. 2B, Supplementary Fig. 6). Trabecular bone volume as a proportion of tissue volume was also significantly decreased in male mice at P70 ($P = 0.018$, Supplementary Fig. 6) and female mice at p183 ($P = 0.002$, Fig. 2).

Long bone BMC was also reduced in *Fubp3*$^{-/-}$ mouse femurs compared to *Fubp3*$^{+/+}$ mice at P21 ($P < 0.05$) and in males at P70 ($P < 0.01$, Supplementary Fig. 7). Additional decreases in BMC were seen in P70 *Fubp3*$^{-/-}$ male tibiae *vs.* *Fubp3*$^{+/+}$ animals ($P < 0.05$, data not shown) and in P183 female *Fubp3*$^{-/-}$ femurs compared to *Fubp3*$^{+/-}$ mice ($P < 0.05$, Fig. 3). Using micro-CT to assess trabecular microarchitecture, P183 female *Fubp3*$^{-/-}$ femurs had significantly decreased bone volume as a proportion of tissue volume ($P = 0.028$, Fig. 3) and significantly increased trabecular spacing ($P = 0.048$, Fig. 3) compared to *Fubp3*$^{+/+}$ mice. Male P183 *Fubp3*$^{-/-}$ mouse femurs had significantly decreased trabecular thickness ($P = 0.032$) compared to *Fubp3*$^{+/+}$ animals. Trabecular parameters were not altered in P70 *Fubp3*$^{-/-}$ mice (Supplementary Fig. 8).

Cortical micro-CT parameters were unchanged in *Fubp3*$^{-/-}$ femurs compared to *Fubp3*$^{+/+}$ femurs at P70 and P183, other than decreases in total area, cortical area and increases in cortical area percentage in P183 female *Fubp3*$^{-/-}$ mice, which may reflect the overall decrease in bone



(caption on next page)

Fig. 1. Effect of *Fubp3* deficiency upon skeletal growth and development. A: Alician blue (cartilage) and alizarin red (bone) staining of *Fubp3*$^{+/+}$ (WT) and *Fubp3*$^{-/-}$ (KO) P1 mouse skeletons. Whole skeleton (top, scale bar 10 mm), and close-up views of forelimb paws (bottom, scale bar 1 mm) and skull (middle, scale bar 1 mm). B: Nose-tail length (left) and caudal vertebral length (right, measured on Faxitron images) of female *Fubp3*$^{+/+}$ (blue), *Fubp3*$^{+/-}$ (green) and *Fubp3*$^{-/-}$ (orange) mice at P21, P70 and P183. Data presented as mean ± standard deviation (SD), analysed by one-way ANOVA with post-hoc Tukey test. C: Mid-tibial sagittal sections from *Fubp3*$^{+/+}$ (WT) and *Fubp3*$^{-/-}$ (KO) at P21 stained with alcian blue and van Gieson to differentiate the cartilaginous growth plate. Top images are 5× magnification of the whole growth plate, middle images are 20× magnification showing the resting zone (RZ), proliferative zone (PZ) and hypertrophic zone (HZ). Bottom graphs show the absolute (left) and relative (right) widths of the total growth plate and growth plate zones. Data presented as mean ± SEM. Scale bar = 100 μm. Significant differences are shown in the overall growth plate width, and widths of the proliferative and hypertrophic zones between *Fubp3*$^{+/+}$ and *Fubp3*$^{-/-}$ mice. ** $P < 0.01$, ***$P < 0.001$. (For interpretation of the references to colour in this figure legend, the reader is referred to the web version of this article.)

size (Fig. 3).

The effect of oestrogen deficiency on lumbar BMC was investigated in *Fubp3*$^{-/-}$ mice who had undergone ovariectomy 6 weeks previously (Supplementary fig. 9). The lowest vertebral BMC is seen in the *Fubp3*$^{-/-}$ mice who had also undergone ovariectomy, followed by the *Fubp3*$^{-/-}$ mice who had undergone sham surgery. The *Fubp3*$^{-/-}$ mice demonstrated significantly lower BMC than their *Fubp3*$^{+/+}$ counterparts, whether in the ovariectomy ($P < 0.001$) or sham surgery ($P < 0.001$) groups.

3.4. *Fubp3 deficiency results in decreased bone strength*

Fubp3 deficient mice had significantly impaired bone strength (Fig. 4), confirming a functional consequence of the decreased BMC and altered microarchitecture seen in mice with *Fubp3* deficiency. L6 vertebrae from P70 male and female *Fubp3*$^{-/-}$ mice had 12–20 % decreases in maximum load compared to wild type mice (male $P = 0.021$, female $P = 0.049$). Furthermore, yield load was reduced by 15–23 % in male and female *Fubp3* deficient L6 lumbar vertebrae at P70 (male $P = 0.019$) and P183 (male $P = 0.008$, female $P = 0.025$), other than in female P70 mice where $P = 0.068$ compared to wild type.

Male and female *Fubp3* deficient femurs also had decreased maximum loads compared to wild type determined by three-point bend testing (Supplementary fig. 10, P70: male $P = 0.012$; P183: male $P = 0.011$, female $P = 0.0009$). Additionally, P70 *Fubp3* deficient male femurs had significantly decreased yield load ($P = 0.004$) and P183 *Fubp3* deficient female femurs had significantly decreased stiffness ($P = 0.028$) compared to wild type (Supplementary fig. 10).

Overall, these data indicate that the reduced BMD and altered trabecular micro-architecture result in decreased bone strength.

3.5. *Effects of Fubp3 deficiency on bone formation and resorption*

Dynamic osteoblastic bone formation was examined in P70 lumbar vertebrae from mice injected with fluorescent calcein at two time points prior to sacrifice. Osteoclast parameters were determined in TRAP-stained tibia sections from P70 mice. No significant differences in osteoblast (mineral apposition rate, bone formation rate or mineralising surface) or osteoclast (osteoclast number, osteoclast surface) parameters were found between *Fubp3* deficient and wild type mice (Supplementary fig. 11A, C). Furthermore, no significant differences in cortical porosity, representing the volume of the canalicular and vascular network, were found between *Fubp3* deficient and wild type femurs (Supplementary fig. 11B).

4. Discussion

To our knowledge, we provide the first phenotype analysis of *Fubp3*$^{-/-}$ mice and demonstrate that *Fubp3* is necessary for normal postnatal skeletal growth and development, and the acquisition and maintenance of normal adult bone mineral content, trabecular microarchitecture and bone strength. These data provide functional characterisation of an important role for *Fubp3* in the developing and adult skeleton, consistent with the hypothesis that *FUBP3* contributes to the association between the 9q34.11 GWAS locus and human BMD, fracture and height.

GWAS have identified over 500 loci associated with BMD and over 700 loci with height, explaining >20 % of the variance of these traits [15,56]. Some of these loci contain clear candidates to explain the association based upon known bone biology or human genetic skeletal disease. Others, such as the association of *FUBP3* with BMD, fracture and height identify novel genes with a previously unidentified role in the skeleton. For these, moving from a novel GWAS association to function can be limited by the currently poor understanding of the non-coding regions of the genome where most associations lie; extended blocks of linkage disequilibrium; and limited tissue specific bioinformatic resources for variant annotation [21,22,57]. This is particularly the case for bone related traits such as BMD which depend upon complex interactions between endocrine, paracrine and biomechanical factors, which are difficult to model accurately *in vitro* and where bone cells are frequently not represented in databases used for functional annotation. *In vivo* studies as presented here are therefore key to validate a gene or variant contributing to the identified association signal and have been successfully applied previously in studies of the skeleton [14,15,58] and other organs [59,60]. Although the GWAS associations at 9q34.11 are clustered in and around *FUBP3*, there are several other genes at the 9q34.11 locus. While genes closest to the GWAS association signal may frequently be causal [15], GWAS associations are known to have the potential to act across large distances and other evidence suggests that the closest gene may not always be causal [61,62]. At other GWAS loci, more than one gene has been shown to influence phenotype [63]. Although our data demonstrate a skeletal role of *Fubp3* which plausibly underlies the association with reduced BMD, fracture and height, our results do not preclude other genes also contributing to the BMD, fracture and height associations at 9q34.11.

The molecular mechanisms and downstream targets by which FUBP3 affects bone function are unknown. The FUBP family of proteins are well characterised as regulators of C-MYC [25,64,65], which is known to have important roles in the skeleton [36–38,66,67]. C-MYC has been shown to be important for chondrocyte proliferation and differentiation necessary for longitudinal bone growth at the growth plate [36,68]. C-MYC is also required for osteoclast/osteoblast proliferation and differentiation [36,67] and is a factor associated with age-related skeletal changes [38]. The current studies demonstrate that *Fubp3* deficiency in mice results in reduced growth plate width, reduced skeletal growth, decreased bone mineral content and reduced bone strength. Future work should be directed to determining whether these result from altered *C-myc* expression because of FUBP3 deficiency or from dysregulation of other FUBP3 regulated pathways. For example, studying the transcriptome in *Fubp3* deficient mice may help to determine the effects of *Fubp3* deficiency, including those relevant to bone. To date only very limited analysis of the effect of FUBP3 deficiency on gene expression is reported in the literature, from microarray analysis of small interfering RNA mediated knockdown of *FUBP3* in human cell lines. However, this indicates a number of potential FUBP3 targets relevant to bone [25]. As FUBP3 is also known to be an RNA binding and regulatory protein [40], combination of transcriptomic with proteomic analysis may be needed for a full assessment of downstream targets of FUBP3.

Previous work has demonstrated that whilst the three FUBP family members have many similarities and may cooperate to regulate expression of target genes such as *C-MYC,* they also have important differences in subcellular localisation, recruitment to *C-MYC* and ability

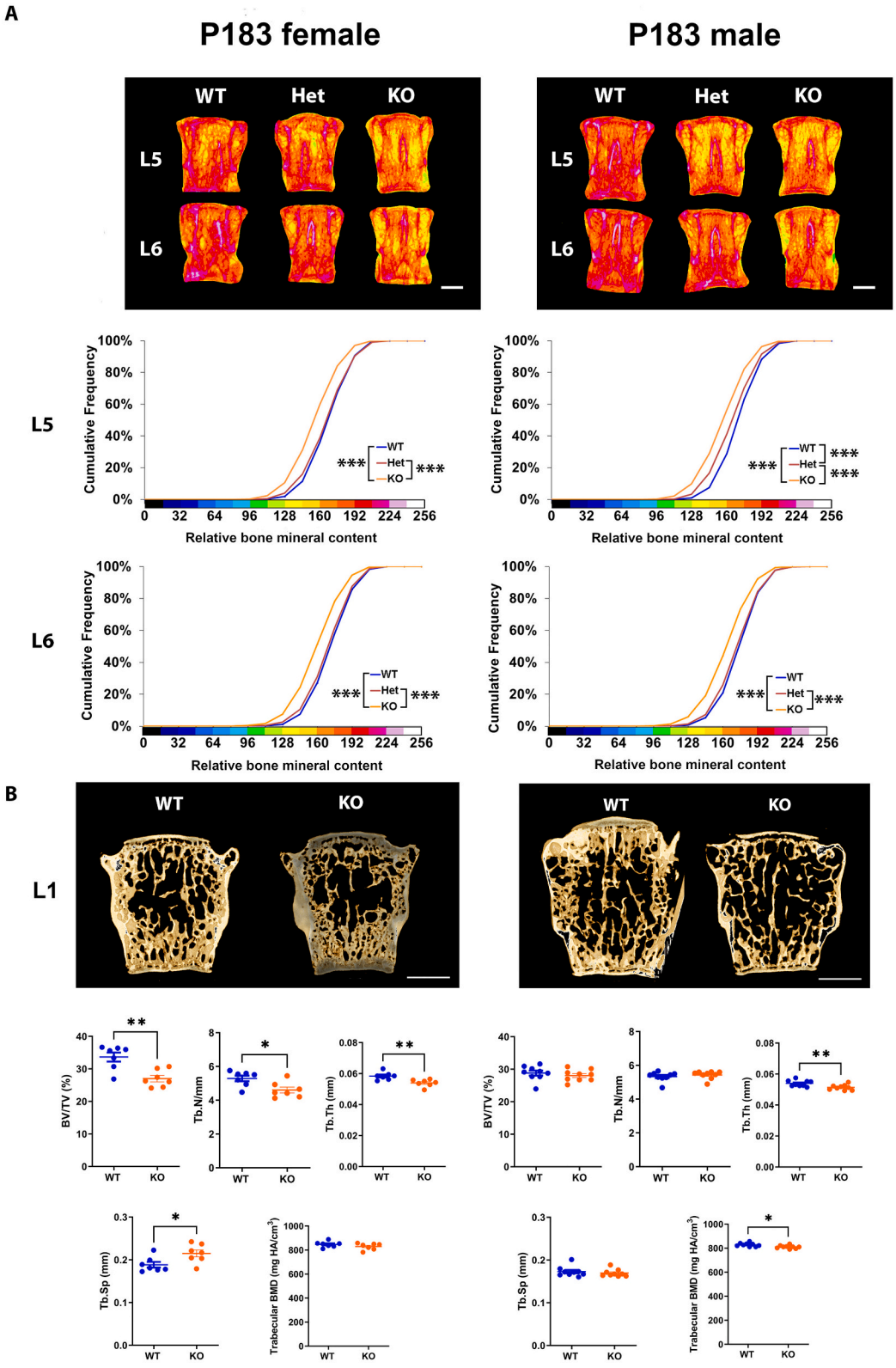


Fig. 2. Lumbar vertebral BMC and structure in *Fubp3*$^{+/+}$, *Fubp3*$^{+/-}$ and *Fubp3*$^{-/-}$ mice at P183. A: Representative 16 colour Faxitron X-ray microradiograph images and cumulative frequency histograms of BMC of the L5 and L6 lumbar vertebrae of *Fubp3*$^{+/+}$ (WT), *Fubp3*$^{+/-}$ (Het) and *Fubp3*$^{-/-}$ (KO) at p183 (blue represents lower BMC, red/orange higher BMC). Scale bar = 1 mm. Kolmogorov-Smirnov test, $n = 5$–10 per group. B: Representative trabecular microCT images of the L1 vertebra and graphs of trabecular microarchitectural parameters of the L1 vertebra. Scale bar = 1 mm. BV/TV: bone volume/tissue volume; Tb.N/mm: trabecular number per mm; Tb.th: trabecular thickness in mm; Tb.Sp: trabecular spacing in mm; trabecular BMD: trabecular bone mineral density. Data analysed by two-tailed *t*-test, * $p < 0.05$, ** $p < 0.01$, ***$p < 0.001$. (For interpretation of the references to colour in this figure legend, the reader is referred to the web version of this article.)

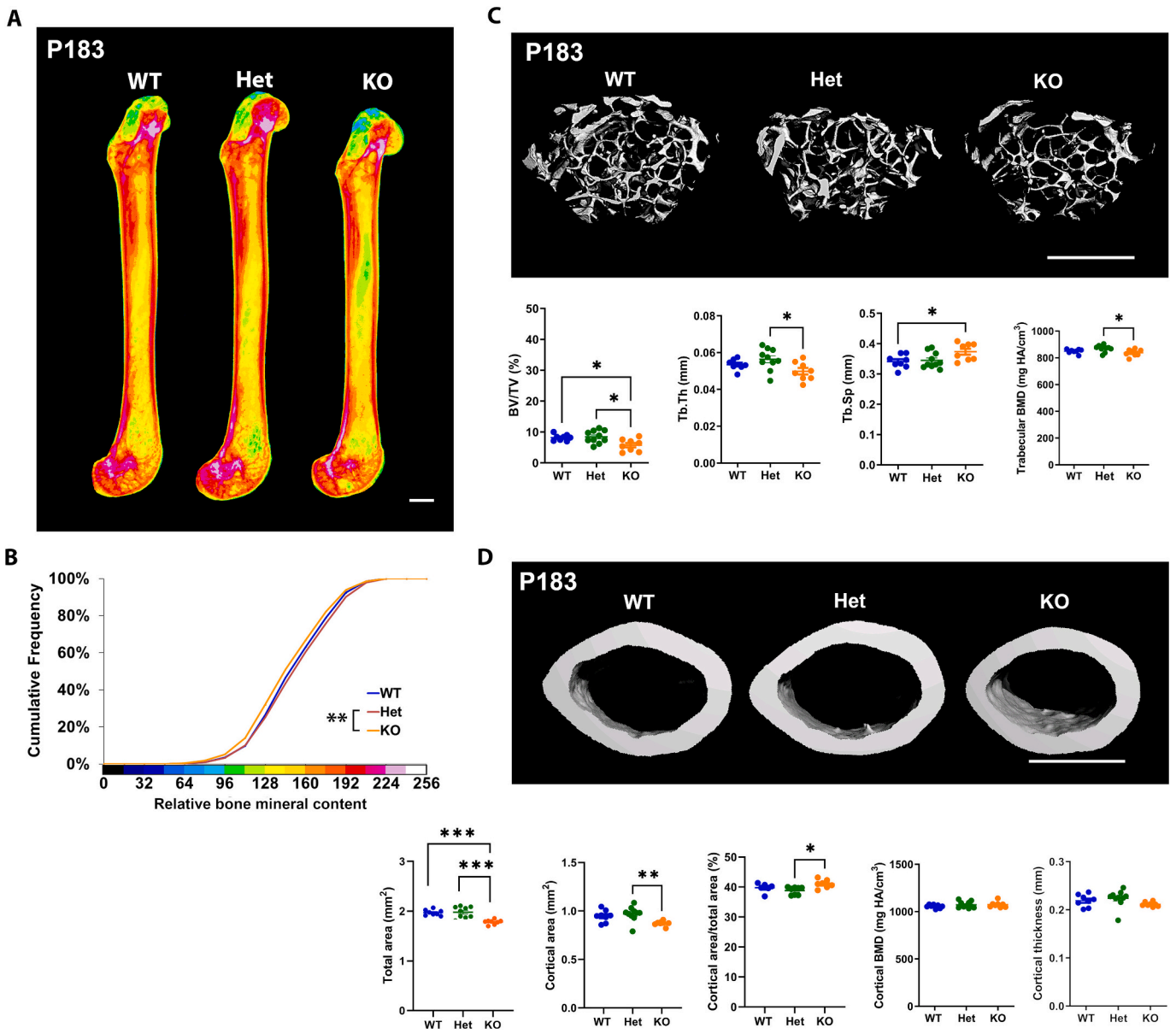


Fig. 3. Long bone structure of *Fubp3*$^{+/+}$, *Fubp3*$^{+/-}$ and *Fubp3*$^{-/-}$ mice at P183. A: Representative 16 colour Faxitron X-ray microradiograph image of femurs of *Fubp3*$^{+/+}$ (WT), *Fubp3*$^{+/-}$ (Het) and *Fubp3*$^{-/-}$ (KO) female mice at P183. Blue pixels represent lower BMC and red/orange represents higher BMC. Scale bar = 1 mm. B: Cumulative frequency histogram of BMC from *Fubp3*$^{+/+}$ (WT), *Fubp3*$^{+/-}$ (Het) and *Fubp3*$^{-/-}$ (KO) female mouse femurs at P183. Kolmogorov-Smirnov test, n = 6–10 per group.

C: Representative trabecular micro-CT images and graphs of trabecular structural parameters of a 1 mm ROI of the distal femur from *Fubp3*$^{+/+}$ (WT), *Fubp3*$^{+/-}$ (Het) and *Fubp3*$^{-/-}$ (KO) female mice at P183. Scale bar 1 mm. Data presented as mean ± SEM. D: Representative cortical micro-CT images and cortical structural parameter graphs from *Fubp3*$^{+/+}$ (WT), *Fubp3*$^{+/-}$ (Het) and *Fubp3*$^{-/-}$ (KO) female mid-femoral cortex at P183. Scale bar 1 mm. Data presented as mean ± SEM. * $p < 0.05$, ** $p < 0.01$, ***$p < 0.001$. (For interpretation of the references to colour in this figure legend, the reader is referred to the web version of this article.)

to stimulate transcription [25,26,69]. Whilst *Fubp1* knockout mice die *in utero* with severe anaemia [30] and *Fubp2* knockout mice survive and reproduce normally [70], *Fubp3*$^{-/-}$ mice are viable and fertile, but they demonstrate a survival deficit with fewer *Fubp3*$^{-/-}$ mice reaching weaning age than the expected Mendelian ratio. The cause of the survival deficit is unclear as unlike *Fubp1* knockouts [30], surviving *Fubp3*$^{-/-}$ mice are grossly morphologically normal. Deficiency of *Fupb2* results in mice with low body weights due to reduced fat mass [71]. In contrast, *Fubp3* deficiency predominately results in short body length, without consistent alterations in weight. Members of the FUBP family have been shown to co-regulate some common targets [25]. It is possible that the lack of other phenotypic features seen in *Fubp3*$^{-/-}$ mice is due to compensatory actions of *Fubp1* and *Fubp2*. Neither *Fubp1* nor *Fubp2* deficient mice have been demonstrated to have an abnormal skeletal phenotype as seen in *Fubp3*$^{-/-}$ mice.

The predominant effect of *Fubp3* deficiency is on vertebral trabecular bone, with lesser impact on long bone cortical BMC or micro-architecture. This may not have been predicted from GWAS, in which the *FUBP3*-containing locus has been associated with femoral neck and lumbar spine BMD as well as heel ultrasound estimated BMD [9,14,15,72,73]. In human osteoporosis, vertebral fractures are the most common osteoporotic fracture and predict fractures at other sites such as the neck of femur [74–76]. Trabecular bone is lost earlier in aging and osteoporosis than cortical bone [77,78] and although mice were studied into adulthood, advanced age was not assessed which may be needed for cortical defects to manifest. Nevertheless, there is precedent that certain

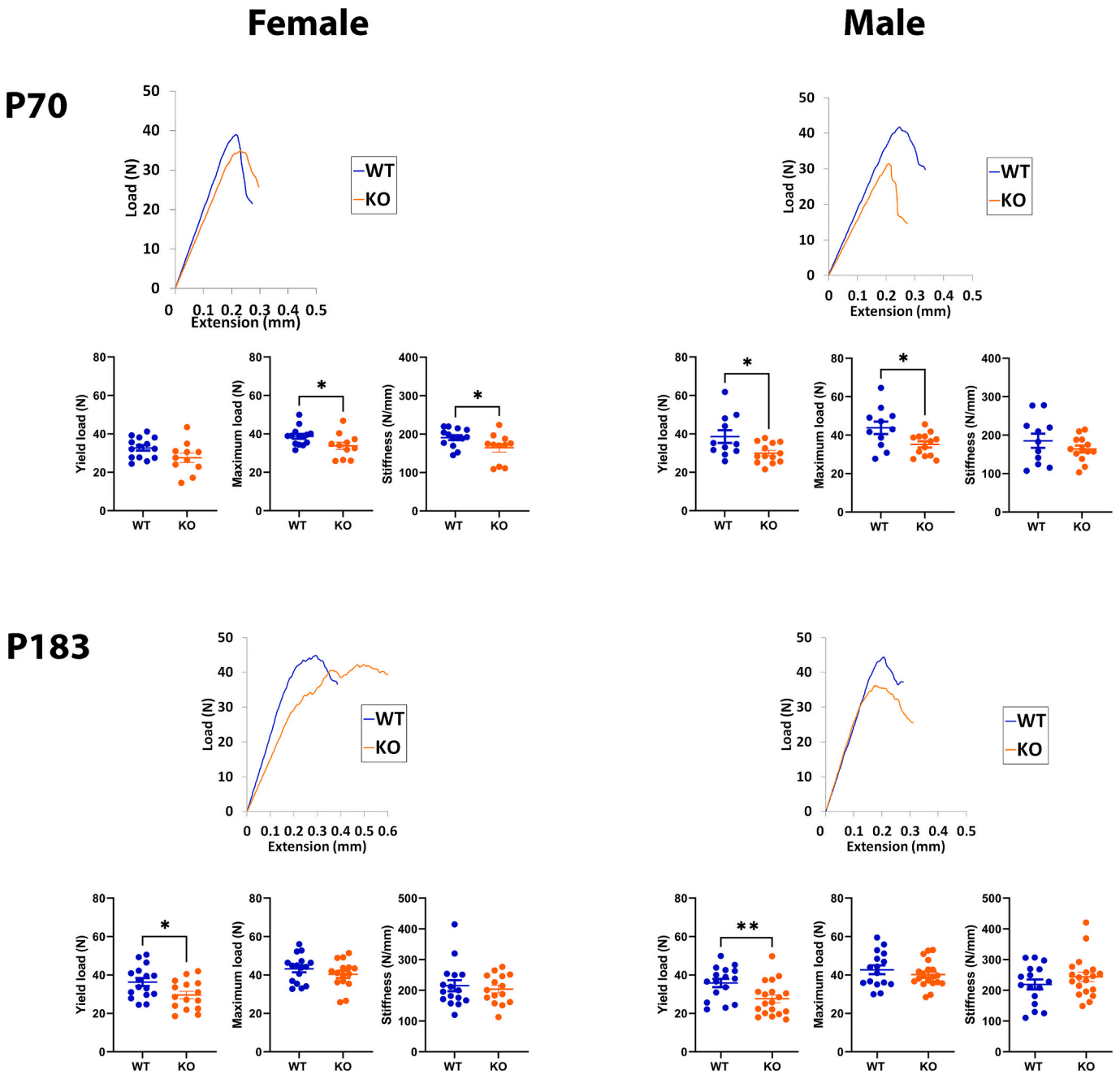


Fig. 4. Vertebral strength of *Fubp3*$^{+/+}$ and *Fubp3*$^{-/-}$ mice at P70 and P183. Representative load-displacement curves of the L6 vertebral body compressed along its proximo-distal axis in female (left) and male (right) in *Fubp3*$^{+/+}$ (WT, blue) and *Fubp3*$^{-/-}$ (KO, orange) mice at P70 (top) and P183 (bottom). Graphs represent yield load, maximum load and stiffness. Data presented as mean ± SEM, two-tailed Student's *t*-test, =11–19 per group. * $p < 0.05$, ** $p < 0.01$. (For interpretation of the references to colour in this figure legend, the reader is referred to the web version of this article.)

signalling pathways can show greater effects upon trabecular bone compared to cortical [79], or effects which differ between skeletal regions. For example, well recognised in the classification of human skeletal dysplasias is that conditions may show different patterns of limb shortening which can be characterised as rhizomelic, affecting the humerus and femur, or mesomelic, referring to shortening of the radius, ulna, tibia or fibula [80]. Disproportionate shortening of the trunk and vertebrae compared to long bones is also recognised in the brachyolmia group of skeletal disorders [81]. *Fubp3* deficiency results in marked shortening of caudal vertebrae, whilst in the hindlimb, long bone shortening affects the tibia, with no effect upon femur length. However, femurs from *Fubp3*$^{-/-}$ mice still showed decreases in strength compared to wild type. Although little is known regarding the downstream effects of FUBP3, FGF9 mRNA has been identified as a potential target of FUBP3 [40]. FGF9 is known to have redundant roles in limb growth and patterning with other FGFs. However, previous data in mice has shown that loss of *Fgf9* causes disproportionate shortening of the femur compared to the tibia [42], the opposite to the pattern demonstrated here. This may suggest that at least some of the actions of FUBP3 on the skeleton can be differentiated from those of FGF9.

Although osteoporosis affects both men and women, it is most common in women following the menopause [82]. Overall, our data do not show clear sexually dimorphic effects of the loss of *Fubp3*, with both male and female mice demonstrating short stature with reduced vertebral BMC. Although female *Fubp3*$^{-/-}$ mice at P183 demonstrated alterations in a greater number of trabecular parameters than male mice of

the same age, both female and male mice showed reduced yield load on biomechanical testing of the L6 vertebra. Mice do not undergo natural menopause in the same way as humans [83], however both ovariectomy and sham treated *Fubp3*$^{-/-}$ mice had lower vertebral BMC than their wild type counterparts and the lowest BMC was seen in *Fubp3*$^{-/-}$ mice who had also undergone ovariectomy. This suggests that *Fubp3* deficiency has effects at least partially independent of and additive to those of oestrogen loss and does not support a sexually dimorphic effect of loss of *Fubp3*.

Although this work suggests that *Fubp3* is needed for normal skeletal growth and adult bone mass in mice, the cellular and molecular mechanisms underlying this are currently unclear and our study has some limitations. Specifically, we were not able to demonstrate either the increased bone resorption or decreased bone formation that would be expected to underlie decreased BMC. Histomorphometric techniques are known to demonstrate large coefficients of variation [84–86]. Although our sample size calculation was based upon previous experience of histomorphometry in our laboratory using femoral samples, the degree of variation seen in the vertebral samples analysed for histomorphometry exceeded that predicted. Therefore, our study may have been underpowered to detect a bone formation or resorption phenotype. Although TRAP staining was attempted on lumbar vertebrae, this proved technically challenging and the results presented for osteoclast histomorphometry are of the tibia, for which protocols are well established. However, as the decreased BMC is predominantly seen in the lumbar vertebrae, this may have prevented detection of a true effect. Assays of bone turnover markers were performed, but gave inconsistent results. Furthermore, although we used a well-established strategy for *Fubp3* knockout and PCR and sequencing confirms cassette insertion into *Fubp3*, we cannot exclude the possibility of additional effects of the cassette upon neighbouring genes also contributing to the phenotype seen.

Future work should seek to establish the mechanisms and pathways through which *Fubp3* has its skeletal effect. In order to further investigate the cellular mechanisms that underlie the phenotype seen, consideration should be given to culture of *Fubp3*$^{-/-}$ bone cells to determine effects upon cell differentiation or function. Electron microscopy would allow characterisation of the ultra-structure of *Fubp3*$^{-/-}$ bones, for example, analysis of micro-mineralisation and resorption pits could provide required information on bone formation and resorption in *Fubp3*$^{-/-}$ mice. As the knockout allele used has conditional potential, future work could also include studying the phenotype of conditional knockout of *Fubp3* in bone relevant cells, whilst analysis of the *Fubp3* deficient transcriptome may determine the key bone relevant pathways by which *Fubp3* has its effect. Nevertheless, the current work demonstrates a role for *Fubp3* in skeletal growth, bone mass and strength, indicating *Fubp3* contributes to the GWAS association at 9q34.11 with BMD, fracture and height.

CRediT authorship contribution statement

Laura M. Watts: Writing – review & editing, Writing – original draft, Project administration, Investigation, Formal analysis, Data curation, Conceptualization. **Penny C. Sparkes:** Writing – review & editing, Investigation, Data curation. **Hannah F. Dewhurst:** Writing – review & editing, Investigation, Data curation. **Siobhan E. Guilfoyle:** Writing – review & editing, Investigation, Data curation. **Andrea S. Pollard:** Writing – review & editing, Supervision, Investigation, Data curation. **Davide Komla-Ebri:** Writing – review & editing, Supervision, Investigation, Data curation. **Natalie C. Butterfield:** Writing – review & editing, Supervision, Methodology, Investigation, Data curation. **Graham R. Williams:** Writing – review & editing, Supervision, Methodology, Investigation, Conceptualization. **J.H. Duncan Bassett:** Writing – review & editing, Supervision, Methodology, Investigation, Conceptualization.

Ethical approval

All experiments were conducted in accordance with the Animals (Scientific Procedures) Act 1986 under appropriate project (PP1540664) and personal licences and additionally approved by the Animal Welfare and Ethical Review Body at Imperial College London.

Funding

This work was funded by a Wellcome Trust 4i Programme Doctoral Clinical Research Fellowship (L.M.W). G.R.W. and J.H.D.B. were funded by a Wellcome Trust Strategic Award (101123) and Wellcome Trust Joint Investigator Award (110140, 110141).

Declaration of competing interest

The authors declare the following financial interests/personal relationships which may be considered as potential competing interests: Laura M Watts reports financial support was provided by Wellcome Trust. J. H. Duncan Bassett reports financial support was provided by Wellcome Trust. Graham R. Williams reports financial support was provided by Wellcome Trust. If there are other authors, they declare that they have no known competing financial interests or personal relationships that could have appeared to influence the work reported in this paper.

Appendix A. Supplementary data

Supplementary data to this article can be found online at https://doi.org/10.1016/j.bone.2025.117472.

Data availability

Data will be made available on request.

References

[1] N.K. Arden, J. Baker, C. Hogg, K. Baan, T.D. Spector, The heritability of bone mineral density, ultrasound of the calcaneus and hip axis length: a study of postmenopausal twins, J. Bone Miner. Res. 11 (2009) 530–534, https://doi.org/10.1002/jbmr.5650110414.

[2] D.M. Smith, W.E. Nance, K.W. Kang, J.C. Christian, C.C. Johnston, Genetic factors in determining bone mass, J. Clin. Invest. 52 (1973) 2800–2808, https://doi.org/10.1172/JCI107476.

[3] K. Silventoinen, S. Sammalisto, M. Perola, D.I. Boomsma, B.K. Cornes, C. Davis, L. Dunkel, M. De Lange, J.R. Harris, J.V.B. Hjelmborg, M. Luciano, N.G. Martin, J. Mortensen, L. Nisticò, N.L. Pedersen, A. Skytthe, T.D. Spector, M.A. Stazi, G. Willemsen, J. Kaprio, Heritability of adult body height: a comparative study of twin cohorts in eight countries, Twin Res. 6 (2003) 399–408, https://doi.org/10.1375/136905203770326402.

[4] E.S. Siris, R. Adler, J. Bilezikian, M. Bolognese, B. Dawson-Hughes, M.J. Favus, S. T. Harris, S.M. Jan de Beur, S. Khosla, N.E. Lane, R. Lindsay, A.D. Nana, E. S. Orwoll, K. Saag, S. Silverman, N.B. Watts, The clinical diagnosis of osteoporosis: a position statement from the National Bone Health Alliance Working Group, Osteoporos. Int. 25 (2014) 1439–1443, https://doi.org/10.1007/s00198-014-2655-z.

[5] T.P. van Staa, E.M. Dennison, H.G. Leufkens, C. Cooper, Epidemiology of fractures in England and Wales, Bone 29 (2001) 517–522.

[6] S.C. Schuit, M. van der Klift, A.E.A. Weel, C.E.D. de Laet, H. Burger, E. Seeman, A. Hofman, A. Uitterlinden, J.P.T. van Leeuwen, H.A. Pols, Fracture incidence and association with bone mineral density in elderly men and women: the Rotterdam study, Bone 34 (2004) 195–202, https://doi.org/10.1016/j.bone.2003.10.001.

[7] O. Johnell, J.A. Kanis, An estimate of the worldwide prevalence and disability associated with osteoporotic fractures, Osteoporos. Int. 17 (2006) 1726–1733, https://doi.org/10.1007/s00198-006-0172-4.

[8] S.R. Cummings, L.J. Melton, Epidemiology and outcomes of osteoporotic fractures, Lancet 359 (2002) 1761–1767, https://doi.org/10.1016/S0140-6736(02)08657-9.

[9] K. Estrada, U. Styrkarsdottir, E. Evangelou, Y.-H. Hsu, E.L. Duncan, E.E. Ntzani, L. Oei, O.M.E. Albagha, N. Amin, J.P. Kemp, D.L. Koller, G. Li, C.-T. Liu, R. L. Minster, A. Moayyeri, L. Vandenput, D. Willner, S.-M. Xiao, L.M. Yerges-Armstrong, H.-F. Zheng, N. Alonso, J. Eriksson, C.M. Kammerer, S.K. Kaptoge, P. J. Leo, G. Thorleifsson, S.G. Wilson, J.F. Wilson, V. Aalto, M. Alen, A.K. Aragaki, T. Aspelund, J.R. Center, Z. Dailiana, D.J. Duggan, M. Garcia, N. Garcia-Giralt, S. Giroux, G. Hallmans, L.J. Hocking, L.B. Husted, K.A. Jameson, R. Khusainova, G. S. Kim, C. Kooperberg, T. Koromila, M. Kruk, M. Laaksonen, A.Z. Lacroix, S.H. Lee,

P.C. Leung, J.R. Lewis, L. Masi, S. Mencej-Bedrac, T.V. Nguyen, X. Nogues, M. S. Patel, J. Prezelj, L.M. Rose, S. Scollen, K. Siggeirsdottir, A.V. Smith, O. Svensson, S. Trompet, O. Trummer, N.M. van Schoor, J. Woo, K. Zhu, S. Balcells, M.L. Brandi, B.M. Buckley, S. Cheng, C. Christiansen, C. Cooper, G. Dedoussis, I. Ford, M. Frost, D. Goltzman, J. González-Macías, M. Kähönen, M. Karlsson, E. Khusnutdinova, J.-M. Koh, P. Kollia, B.L. Langdahl, W.D. Leslie, P. Lips, O. Ljunggren, R.S. Lorenc, J. Marc, D. Mellstrom, B. Obermayer-Pietsch, J.M. Olmos, U. Pettersson-Kymmer, D.M. Reid, J.A. Riancho, P.M. Ridker, F. Rousseau, P.E.S. Lagboom, N.L.S. Tang, R. Urreizti, W. Van Hul, J. Viikari, M.T. Zarrabeitia, Y.S. Aulchenko, M. Castano-Betancourt, E. Grundberg, L. Herrera, T. Ingvarsson, H. Johannsdottir, T. Kwan, R. Li, R. Luben, C. Medina-Gómez, S. Th Palsson, S. Reppe, J.I. Rotter, G. Sigurdsson, J.B.J. van Meurs, D. Verlaan, F.M.K. Williams, A.R. Wood, Y. Zhou, K.M. Gautvik, T. Pastinen, S. Raychaudhuri, J.A. Cauley, D.I. Chasman, G.R. Clark, S.R. Cummings, P. Danoy, E.M. Dennison, R. Eastell, J.A. Eisman, V. Gudnason, A. Hofman, R.D. Jackson, G. Jones, J.W. Jukema, K.-T. Khaw, T. Lehtimäki, Y. Liu, M. Lorentzon, E. McCloskey, B.D. Mitchell, K. Nandakumar, G.C. Nicholson, B. A. Oostra, M. Peacock, H.A.P. Pols, R.L. Prince, O. Raitakari, I.R. Reid, J. Robbins, P.N. Sambrook, P.C. Sham, A.R. Shuldiner, F.A. Tylavsky, C.M. van Duijn, N. J. Wareham, L.A. Cupples, M.J. Econs, D.M. Evans, T.B. Harris, A.W.C. Kung, B. M. Psaty, J. Reeve, T.D. Spector, E.A. Streeten, M.C. Zillikens, U. Thorsteinsdottir, C. Ohlsson, D. Karasik, J.B. Richards, M.A. Brown, K. Stefansson, A.G. Uitterlinden, S.H. Ralston, J.P.A. Ioannidis, D.P. Kiel, F. Rivadeneira, Genome-wide meta-analysis identifies 56 bone mineral density loci and reveals 14 loci associated with risk of fracture, Nat. Genet. 44 (2012) 491–501, https://doi.org/10.1038/ng.2249.

[10] J.P. Kemp, C. Medina-Gomez, K. Estrada, B. St Pourcain, D.H.M. Heppe, N. M. Warrington, L. Oei, S.M. Ring, C.J. Kruithof, N.J. Timpson, L.E. Wolber, S. Reppe, K. Gautvik, E. Grundberg, B. Ge, B. van der Eerden, J. van de Peppel, M. A. Hibbs, C.L. Ackert-Bicknell, K. Choi, D.L. Koller, M.J. Econs, F.M.K. Williams, T. Foroud, M. Carola Zillikens, C. Ohlsson, A. Hofman, A.G. Uitterlinden, G. Davey Smith, V.W.V. Jaddoe, J.H. Tobias, F. Rivadeneira, D.M. Evans, Phenotypic dissection of bone mineral density reveals skeletal site specificity and facilitates the identification of novel loci in the genetic regulation of bone mass attainment, PLoS Genet. 10 (2014) e1004423, https://doi.org/10.1371/journal.pgen.1004423.

[11] I. Galván-Femenía, M. Obón-Santacana, D. Piñeyro, M. Guindo-Martinez, X. Duran, A. Carreras, R. Pluvinet, J. Velasco, L. Ramos, S. Aussó, J.M. Mercader, L. Puig, M. Perucho, D. Torrents, V. Moreno, L. Sumoy, R. de Cid, Multitrait genome association analysis identifies new susceptibility genes for human anthropometric variation in the GCAT cohort, J. Med. Genet. 55 (2018) 765–778, https://doi.org/10.1136/jmedgenet-2018-105437.

[12] L. Yengo, S. Vedantam, E. Marouli, J. Sidorenko, E. Bartell, S. Sakaue, M. Graff, A. U. Eliasen, Y. Jiang, S. Raghavan, J. Miao, J.D. Arias, S.E. Graham, R.E. Mukamel, C.N. Spracklen, X. Yin, S.-H. Chen, T. Ferreira, H.H. Highland, Y. Ji, T. Karaderi, K. Lin, K. Lüll, D.E. Malden, C. Medina-Gomez, M. Machado, A. Moore, S. Rüeger, X. Sim, S. Vrieze, T.S. Ahluwalia, M. Akiyama, M.A. Allison, M. Alvarez, M.K. Andersen, *A. Ani*, V. Appadurai, L. Arbeeva, S. Bhaskar, L.F. Bielak, S. Bollepalli, L. L. Bonnycastle, J. Bork-Jensen, J.P. Bradfield, Y. Bradford, P.S. Braund, J.A. Brody, K.S. Burgdorf, B.E. Cade, H. Cai, Q. Cai, A. Campbell, M. Cañadas-Garre, E. Catamo, J.-F. Chai, X. Chai, L.-C. Chang, Y.-C. Chang, C.-H. Chen, A. Chesi, S.H. Choi, R.-H. Chung, M. Cocca, M.P. Concas, C. Couture, G. Cuellar-Partida, R. Danning, E.W. Daw, F. Degenhard, G.E. Delgado, A. Delitala, A. Demirkan, X. Deng, P. Devineni, A. Dietl, M. Dimitriou, L. Dimitrov, R. Dorajoo, A.B. Ekici, J.E. Engmann, Z. Fairhurst-Hunter, A.-E. Farmaki, J.D. Faul, J.-C. Fernandez-Lopez, L. Forer, M. Francescatto, S. Freitag-Wolf, C. Fuchsberger, T.E. Galesloot, Y. Gao, Z. Gao, F. Geller, O. Giannakopoulou, F. Giulianini, A.P. Gjesing, A. Goel, S.D. Gordon, M. Gorski, J. Grove, X. Guo, S. Gustafsson, J. Haessler, T.F. Hansen, A.S. Havulinna, S.J. Haworth, J. He, N. Heard-Costa, P. Hebbar, G. Hindy, Y.-L.A. Ho, E. Hofer, E. Holliday, K. Horn, W.E. Hornsby, J.-J. Hottenga, H. Huang, J. Huang, A. Huerta-Chagoya, J.E. Huffman, Y.-J. Hung, S. Huo, M.Y. Hwang, H. Iha, D.D. Ikeda, M. Isono, A.U. Jackson, S. Jäger, I.E. Jansen, I. Johansson, J.B. Jonas, A. Jonsson, T. Jørgensen, I.-P. Kalafati, M. Kanai, S. Kanoni, L.L. Kårhus, A. Kasturiratne, T. Katsuya, T. Kawaguchi, R.L. Kember, K.A. Kentistou, H.-N. Kim, Y. J. Kim, M.E. Kleber, M.J. Knol, A. Kurbasic, M. Lauzon, P. Le, R. Lea, J.-Y. Lee, H.L. Leonard, S.A. Li, X. Li, X. Li, J. Liang, H. Lin, S.-Y. Lin, J. Liu, X. Liu, K.S. Lo, J. Long, L. Lores-Motta, J. Luan, V. Lyssenko, L.-P. Lyytikäinen, A. Mahajan, V. Mamakou, M. Mangino, A. Manichaikul, J. Marten, M. Mattheisen, L. Mavarani, A. F. McDaid, K. Meidtner, T.L. Melendez, J.M. Mercader, Y. Milaneschi, J.E. Miller, I. Y. Millwood, P.P. Mishra, R.E. Mitchell, L.T. Møllehave, A. Morgan, S. Mucha, M. Munz, M. Nakatochi, C.P. Nelson, M. Nethander, C.W. Nho, A.A. Nielsen, I.M. Nolte, S.S. Nongmaithem, R. Noordam, I. Ntalla, T. Nutile, A. Pandit, P. Christofidou, K. Pärna, M. Pauper, E.R.B. Petersen, L. V Petersen, N. Pitkänen, O. Polašek, A. Poveda, M.H. Preuss, S. Pyarajan, L.M. Raffield, H. Rakugi, J. Ramirez, A. Rasheed, D. Raven, N.W. Rayner, C. Riveros, R. Rohde, D. Ruggiero, S.E. Ruotsalainen, K.A. Ryan, M. Sabater-Lleal, R. Saxena, M. Scholz, A. Sendamarai, B. Shen, J. Shi, J.H. Shin, C. Sidore, C.M. Sitlani, R.C. Slieker, R.A.J. Smit, A. V Smith, J.A. Smith, L.J. Smyth, L. Southam, V. Steinthorsdottir, L. Sun, F. Takeuchi, D.S.P. Tallapragada, K.D. Taylor, B.O. Tayo, C. Tcheandjieu, N. Terzikhan, P. Tesolin, A. Teumer, E. Theusch, D.J. Thompson, G. Thorleifsson, P.R.H.J. Timmers, S. Trompet, C. Turman, S. Vaccargiu, S.W. van der Laan, P.J. van der Most, J.B. van Klinken, J. van Setten, S.S. Verma, N. Verweij, Y. Veturi, C.A. Wang, C. Wang, L. Wang, Z. Wang, H.R. Warren, W. Bin Wei, A.R. Wickremasinghe, M. Wielscher, K. L. Wiggins, B.S. Winsvold, A. Wong, Y. Wu, M. Wuttke, R. Xia, T. Xie, K. Yamamoto, J. Yang, J. Yao, H. Young, N.A. Yousri, L. Yu, L. Zeng, W. Zhang, X. Zhang, J.-H. Zhao, W. Zhao, W. Zhou, M.E. Zimmermann, M. Zoledziewska, L.S. Adair, H.H.H. Adams, C.A. Aguilar-Salinas, F. Al-Mulla, D.K. Arnett, F.W. Asselbergs, B.O. Åsvold, J. Attia, B. Banas, S. Bandinelli, D.A. Bennett, T. Bergler, D. Bharadwaj, G. Biino, H. Bisgaard, E. Boerwinkle, C.A. Böger, K. Bønnelykke, D.I. Boomsma, A.D. Børglum, J.B. Borja, C. Bouchard, D.W. Bowden, I. Brandslund, B. Brumpton, J.E. Buring, M.J. Caulfield, J.C. Chambers, G.R. Chandak, S.J. Chanock, N. Chaturvedi, Y.-D.I. Chen, Z. Chen, C.-Y. Cheng, I.E. Christophersen, M. Ciullo, J. W. Cole, F.S. Collins, R.S. Cooper, M. Cruz, F. Cucca, L.A. Cupples, M.J. Cutler, S.M. Damrauer, T.M. Dantoft, G.J. de Borst, L.C.P.G.M. de Groot, P.L. De Jager, D.P. V de Kleijn, H. Janaka de Silva, G. V Dedoussis, A.I. den Hollander, S. Du, D.F. Easton, P.J.M. Elders, A.H. Eliassen, P.T. Ellinor, S. Elmståhl, J. Erdmann, M.K. Evans, D. Fatkin, B. Feenstra, M.F. Feitosa, L. Ferrucci, I. Ford, M. Fornage, A. Franke, P.W. Franks, B.I. Freedman, P. Gasparini, C. Gieger, G. Girotto, M.E. Goddard, Y.M. Golightly, C. Gonzalez-Villalpando, P. Gordon-Larsen, H. Grallert, S. F.A. Grant, N. Grarup, L. Griffiths, V. Gudnason, C. Haiman, H. Hakonarson, T. Hansen, C.A. Hartman, A.T. Hattersley, C. Hayward, S.R. Heckbert, C.-K. Heng, C. Hengstenberg, A.W. Hewitt, H. Hishigaki, C.B. Hoyng, P.L. Huang, W. Huang, S.C. Hunt, K. Hveem, E. Hyppönen, W.G. Iacono, S. Ichihara, M.A. Ikram, C.R. Isasi, R. D. Jackson, M.-R. Jarvelin, Z.-B. Jin, K.-H. Jöckel, P.K. Joshi, P. Jousilahti, J.W. Jukema, M. Kähönen, Y. Kamatani, K.D. Kang, J. Kaprio, S.L.R. Kardia, F. Karpe, N. Kato, F. Kee, T. Kessler, A. V Khera, C.C. Khor, L.A.L.M. Kiemeney, B.-J. Kim, E.K. Kim, H.-L. Kim, P. Kirchhof, M. Kivimaki, W.-P. Koh, H.A. Koistinen, G.D. Kolovou, J.S. Kooner, C. Kooperberg, A. Köttgen, P. Kovacs, A. Kraaijeveld, P. Kraft, R.M. Krauss, M. Kumari, Z. Kutalik, M. Laakso, L.A. Lange, C. Langenberg, L.J. Launer, L. Le Marchand, H. Lee, N.R. Lee, T. Lehtimäki, H. Li, L. Li, W. Lieb, X. Lin, L. Lind, A. Linneberg, C.-T. Liu, J. Liu, M. Loeffler, B. London, S.A. Lubitz, S.J. Lye, D.A. Mackey, R. Mägi, P.K.E. Magnusson, G.M. Marcus, P.M. Vidal, N.G. Martin, W. März, F. Matsuda, R.W. McGarrah, M. McGue, A.J. McKnight, S.E. Medland, D. Mellström, A. Metspalu, B.D. Mitchell, P. Mitchell, D.O. Mook-Kanamori, A.D. Morris, L.A. Mucci, P.B. Munroe, M.A. Nalls, S. Nazarian, A.E. Nelson, M.J. Neville, C. Newton-Cheh, C.S. Nielsen, M.M. Nöthen, C. Ohlsson, A.J. Oldehinkel, L. Orozco, K. Pahkala, P. Pajukanta, C.N.A. Palmer, E.J. Parra, C. Pattaro, O. Pedersen, C.E. Pennell, B.W.J.H. Penninx, L. Perusse, A. Peters, P.A. Peyser, D.J. Porteous, D. Posthuma, C. Power, P.P. Pramstaller, M.A. Province, Q. Qi, J. Qu, D. J. Rader, O.T. Raitakari, S. Ralhan, L.S. Rallidis, D.C. Rao, S. Redline, D.F. Reilly, A. P. Reiner, S.Y. Rhee, P.M. Ridker, M. Rienstra, S. Ripatti, M.D. Ritchie, D.M. Roden, F.R. Rosendaal, J.I. Rotter, I. Rudan, F. Rutters, C. Sabanayagam, D. Saleheen, V. Salomaa, N.J. Samani, D.K. Sanghera, N. Sattar, B. Schmidt, H. Schmidt, R. Schmidt, M.B. Schulze, H. Schunkert, L.J. Scott, R.J. Scott, P. Sever, E.J. Shiroma, M.B. Shoemaker, X.-O. Shu, E.M. Simonsick, M. Sims, J.R. Singh, A.B. Singleton, M. F. Sinner, J.G. Smith, H. Snieder, T.D. Spector, M.J. Stampfer, K.J. Stark, D.P. Strachan, L.M. 't Hart, Y. Tabara, H. Tang, J.-C. Tardif, T.A. Thanaraj, N.J. Timpson, A. Tönjes, A. Tremblay, T. Tuomi, J. Tuomilehto, M.-T. Tusié-Luna, A.G. Uitterlinden, R.M. van Dam, P. van der Harst, N. Van der Velde, C.M. van Duijn, N. M. van Schoor, V. Vitart, U. Völker, P. Vollenweider, H. Völzke, N.H. Wacher-Rodarte, M. Walker, Y.X. Wang, N.J. Wareham, R.M. Watanabe, H. Watkins, D.R. Weir, T.M. Werge, E. Widen, L.R. Wilkens, G. Willemsen, W.C. Willett, J.F. Wilson, T.-Y. Wong, J.-T. Woo, A.F. Wright, J.-Y. Wu, H. Xu, C.S. Yajnik, M. Yokota, J.-M. Yuan, E. Zeggini, B.S. Zemel, W. Zheng, X. Zhu, J.M. Zmuda, A.B. Zonderman, J.-A. Zwart, 23andMe Research Team, VA Million Veteran Program, DiscovEHR (DiscovEHR and MyCode Community Health Initiative), eMERGE (Electronic Medical Records and Genomics Network), Lifelines Cohort Study, PRACTICAL Consortium, Understanding Society Scientific Group, D.I. Chasman, Y.S. Cho, I.M. Heid, M.I. McCarthy, M.C.Y. Ng, C.J. O'Donnell, F. Rivadeneira, U. Thorsteinsdottir, Y. V Sun, E.S. Tai, M. Boehnke, P. Deloukas, A.E. Justice, C.M. Lindgren, R.J.F. Loos, K.L. Mohlke, K.E. North, K. Stefansson, R.G. Walters, T.W. Winkler, K.L. Young, P.-R. Loh, J. Yang, T. Esko, T.L. Assimes, A. Auton, G.R. Abecasis, C.J. Willer, A.E. Locke, S.I. Berndt, G. Lettre, T.M. Frayling, Y. Okada, A. R. Wood, P.M. Visscher, J.N. Hirschhorn, A saturated map of common genetic variants associated with human height., Nature 610 (2022) 704–712. doi:https://doi.org/10.1038/s41586-022-05275-y.

[13] C. Medina-gomez, J.P. Kemp, K. Trajanoska, J. Luan, A. Chesi, T.S. Ahluwalia, D. O. Mook-kanamori, A. Ham, K. Zhu, M. Atalay, C. Liu, M. Nethander, L. Broer, G. Porleifsson, B.H. Mullin, S.K. Handelman, M.A. Nalls, L.E. Jessen, D.H. M. Heppe, J.B. Richards, C. Wang, B. Chawes, K.E. Schraut, N. Amin, N. Wareham, D. Karasik, N. Van Der Velde, Life-course genome-wide association study meta-analysis of total body BMD and assessment of age-specific effects, Am. J. Hum. Genet. 102 (2018) 88–102, https://doi.org/10.1016/j.ajhg.2017.12.005.

[14] J.P. Kemp, J.A. Morris, C. Medina-Gomez, V. Forgetta, N.M. Warrington, S. E. Youlten, J. Zheng, C.L. Gregson, E. Grundberg, K. Trajanoska, J.G. Logan, A. S. Pollard, P.C. Sparkes, E.J. Ghirardello, R. Allen, V.D. Leitch, N.C. Butterfield, D. Komla-Ebri, A.-T. Adoum, K.F. Curry, J.K. White, F. Kussy, K.M. Greenlaw, C. Xu, N.C. Harvey, C. Cooper, D.J. Adams, C.M.T. Greenwood, M.T. Maurano, S. Kaptoge, F. Rivadeneira, J.H. Tobias, P.I. Croucher, C.L. Ackert-Bicknell, J.H. D. Bassett, G.R. Williams, J.B. Richards, D.M. Evans, Identification of 153 new loci associated with heel bone mineral density and functional involvement of GPC6 in osteoporosis, Nat. Genet. 49 (2017) 1468–1475, https://doi.org/10.1038/ng.3949.

[15] J.A. Morris, J.P. Kemp, S.E. Youlten, L. Laurent, J.G. Logan, R.C. Chai, N. A. Vulpescu, V. Forgetta, A. Kleinman, S.T. Mohanty, C.M. Sergio, J. Quinn, L. Nguyen-Yamamoto, A.-L. Luco, J. Vijay, M.-M. Simon, A. Pramatarova, C. Medina-Gomez, K. Trajanoska, E.J. Ghirardello, N.C. Butterfield, K.F. Curry, V. D. Leitch, P.C. Sparkes, A.-T. Adoum, N.S. Mannan, D.S.K. Komla-Ebri, A.S. Pollard, H.F. Dewhurst, T.A.D. Hassall, M.-J.G. Beltejar, 23andMe Research Team, D. J. Adams, S.M. Vaillancourt, S. Kaptoge, P. Baldock, C. Cooper, J. Reeve, E. E. Ntzani, E. Evangelou, C. Ohlsson, D. Karasik, F. Rivadeneira, D.P. Kiel, J. H. Tobias, C.L. Gregson, N.C. Harvey, E. Grundberg, D. Goltzman, D.J. Adams, C. J. Lelliott, D.A. Hinds, C.L. Ackert-Bicknell, Y.-H. Hsu, M.T. Maurano, P. I. Croucher, G.R. Williams, J.H.D. Bassett, D.M. Evans, J.B. Richards, An atlas of genetic influences on osteoporosis in humans and mice, Nat. Genet. 51 (2019) 258–266, https://doi.org/10.1038/s41588-018-0302-x.

[16] K. Trajanoska, J.A. Morris, L. Oei, H.-F. Zheng, D.M. Evans, D.P. Kiel, C. Ohlsson, J. B. Richards, F. Rivadeneira, Assessment of the genetic and clinical determinants of fracture risk: genome wide association and mendelian randomisation study, BMJ (2018) k3225, https://doi.org/10.1136/bmj.k3225.

[17] S.K. Kim, Identification of 613 new loci associated with heel bone mineral density and a polygenic risk score for bone mineral density, osteoporosis and fracture, PLoS One 13 (2018) e0200785, https://doi.org/10.1371/journal.pone.0200785.

[18] H. Lango Allen, K. Estrada, G. Lettre, S.I. Berndt, M.N. Weedon, F. Rivadeneira, C. J. Willer, A.U. Jackson, S. Vedantam, S. Raychaudhuri, T. Ferreira, A.R. Wood, R. J. Weyant, A.V. Segrè, E.K. Speliotes, E. Wheeler, N. Soranzo, J.-H. Park, J. Yang, D. Gudbjartsson, N.L. Heard-Costa, J.C. Randall, L. Qi, A. Vernon Smith, R. Mägi, T. Pastinen, L. Liang, I.M. Heid, J. Luan, G. Thorleifsson, T.W. Winkler, M. E. Goddard, K. Sin Lo, C. Palmer, T. Workalemahu, Y.S. Aulchenko, Å. Johansson, M. Carola Zillikens, M.F. Feitosa, T. Esko, T. Johnson, S. Ketkar, P. Kraft, M. Mangino, I. Prokopenko, D. Absher, E. Albrecht, F. Ernst, N.L. Glazer, C. Hayward, J.-J. Hottenga, K.B. Jacobs, J.W. Knowles, Z. Kutalik, K.L. Monda, O. Polasek, M. Preuss, N.W. Rayner, N.R. Robertson, V. Steinthorsdottir, J.P. Tyrer, B.F. Voight, F. Wiklund, J. Xu, J. Hua Zhao, D.R. Nyholt, N. Pellikka, M. Perola, J. R.B. Perry, I. Surakka, M.-L. Tammesoo, E.L. Altmaier, N. Amin, T. Aspelund, T. Bhangale, G. Boucher, D.I. Chasman, C. Chen, L. Coin, M.N. Cooper, A.L. Dixon, Q. Gibson, E. Grundberg, K. Hao, M. Juhani Junttila, L.M. Kaplan, J. Kettunen, I. R. König, T. Kwan, R.W. Lawrence, D.F. Levinson, M. Lorentzon, B. McKnight, A. P. Morris, M. Müller, J. Suh Ngwa, S. Purcell, S. Rafelt, R.M. Salem, E. Salvi, S. Sanna, J. Shi, U. Sovio, J.R. Thompson, M.C. Turchin, L. Vandenput, D. J. Verlaan, V. Vitart, C.C. White, A. Ziegler, P. Almgren, A.J. Balmforth, H. Campbell, L. Citterio, A. De Grandi, A. Dominiczak, J. Duan, P. Elliott, R. Elosua, J.G. Eriksson, N.B. Freimer, E.J.C. Geus, N. Glorioso, S. Haiqing, A.-L. Hartikainen, A.S. Havulinna, A.A. Hicks, J. Hui, W. Igl, T. Illig, A. Jula, E. Kajantie, T. O. Kilpeläinen, M. Koiranen, I. Kolcic, S. Koskinen, P. Kovacs, J. Laitinen, J. Liu, M.-L. Lokki, A. Marusic, A. Maschio, T. Meitinger, A. Mulas, G. Paré, A.N. Parker, J. F. Peden, A. Petersmann, I. Pichler, K.H. Pietiläinen, A. Pouta, M. Ridderstråle, J. I. Rotter, J.G. Sambrook, A.R. Sanders, C. Oliver Schmidt, J. Sinisalo, J.H. Smit, H. M. Stringham, G. Bragi Walters, E. Widen, S.H. Wild, G. Willemsen, L. Zagato, L. Zgaga, P. Zitting, H. Alavere, M. Farrall, W.L. McArdle, M. Nelis, M.J. Peters, S. Ripatti, J.B.J. van Meurs, K.K. Aben, K.G. Ardlie, J.S. Beckmann, J.P. Beilby, R. N. Bergman, S. Bergmann, F.S. Collins, D. Cusi, M. den Heijer, G. Eiriksdottir, P. V. Gejman, A.S. Hall, A. Hamsten, H.V. Huikuri, C. Iribarren, M. Kähönen, J. Kaprio, S. Kathiresan, L. Kiemeney, T. Kocher, L.J. Launer, T. Lehtimäki, O. Melander, T.H. Mosley Jr., A.W. Musk, M.S. Nieminen, C.J. O'Donnell, C. Ohlsson, B. Oostra, L.J. Palmer, O. Raitakari, P.M. Ridker, J.D. Rioux, A. Rissanen, C. Rivolta, H. Schunkert, A.R. Shuldiner, D.S. Siscovick, M. Stumvoll, A. Tönjes, J. Tuomilehto, G.-J. van Ommen, J. Viikari, A.C. Heath, N.G. Martin, G. W. Montgomery, M.A. Province, M. Kayser, A.M. Arnold, L.D. Atwood, E. Boerwinkle, S.J. Chanock, P. Deloukas, C. Gieger, H. Grönberg, P. Hall, A. T. Hattersley, C. Hengstenberg, W. Hoffman, G. Mark Lathrop, V. Salomaa, S. Schreiber, M. Uda, D. Waterworth, A.F. Wright, T.L. Assimes, I. Barroso, A. Hofman, K.L. Mohlke, D.I. Boomsma, M.J. Caulfield, L. Adrienne Cupples, J. Erdmann, C.S. Fox, V. Gudnason, U. Gyllensten, T.B. Harris, R.B. Hayes, M.-R. Jarvelin, V. Mooser, P.B. Munroe, W.H. Ouwehand, B.W. Penninx, P. P. Pramstaller, T. Quertermous, I. Rudan, N.J. Samani, T.D. Spector, H. Völzke, H. Watkins, J.F. Wilson, L.C. Groop, T. Haritunians, F.B. Hu, R.C. Kaplan, A. Metspalu, K.E. North, D. Schlessinger, N.J. Wareham, D.J. Hunter, J. R. O'Connell, D.P. Strachan, H.-E. Wichmann, I.B. Borecki, C.M. van Duijn, E. E. Schadt, U. Thorsteinsdottir, L. Peltonen, A.G. Uitterlinden, P.M. Visscher, N. Chatterjee, R.J.F. Loos, M. Boehnke, M.I. McCarthy, E. Ingelsson, C.M. Lindgren, G.R. Abecasis, K. Stefansson, T.M. Frayling, J.N. Hirschhorn, Hundreds of variants clustered in genomic loci and biological pathways affect human height, Nature 467 (2010) 832–838, https://doi.org/10.1038/nature09410.

[19] A.R. Wood, T. Esko, J. Yang, S. Vedantam, T.H. Pers, S. Gustafsson, A.Y. Chu, K. Estrada, J. Luan, Z. Kutalik, N. Amin, M.L. Buchkovich, D.C. Croteau-Chonka, F. R. Day, Y. Duan, T. Fall, R. Fehrmann, T. Ferreira, A.U. Jackson, J. Karjalainen, K. S. Lo, A.E. Locke, R. Mägi, E. Mihailov, E. Porcu, J.C. Randall, A. Scherag, A.A. E. Vinkhuyzen, H.-J. Westra, T.W. Winkler, T. Workalemahu, J.H. Zhao, D. Absher, E. Albrecht, D. Anderson, J. Baron, M. Beekman, A. Demirkan, G.B. Ehret, B. Feenstra, M.F. Feitosa, K. Fischer, R.M. Fraser, A. Goel, J. Gong, A.E. Justice, S. Kanoni, M.E. Kleber, K. Kristiansson, U. Lim, V. Lotay, J.C. Lui, M. Mangino, I. M. Leach, C. Medina-Gomez, M.A. Nalls, D.R. Nyholt, C.D. Palmer, D. Pasko, S. Pechlivanis, I. Prokopenko, J.S. Ried, S. Ripke, D. Shungin, A. Stancáková, R. J. Strawbridge, Y.J. Sung, T. Tanaka, A. Teumer, S. Trompet, S.W. van der Laan, J. van Setten, J.V. Van Vliet-Ostaptchouk, Z. Wang, L. Yengo, W. Zhang, U. Afzal, J. Ärnlöv, G.M. Arscott, S. Bandinelli, A. Barrett, C. Bellis, A.J. Bennett, C. Berne, M. Blüher, J.L. Bolton, Y. Böttcher, H.A. Boyd, M. Bruinenberg, B.M. Buckley, S. Buyske, I.H. Caspersen, P.S. Chines, R. Clarke, S. Claudi-Boehm, M. Cooper, E. W. Daw, P.A. De Jong, J. Deelen, G. Delgado, J.C. Denny, R. Dhonukshe-Rutten, M. Dimitriou, A.S.F. Doney, M. Dörr, N. Eklund, E. Eury, L. Folkersen, M.E. Garcia, F. Geller, V. Giedraitis, A.S. Go, H. Grallert, T.B. Grammer, J. Gräßler, H. Grönberg, L.C.P.G.M. de Groot, C.J. Groves, J. Haessler, P. Hall, T. Haller, G. Hallmans, A. Hannemann, C.A. Hartman, M. Hassinen, C. Hayward, N.L. Heard-Costa, Q. Helmer, G. Hemani, A.K. Henders, H.L. Hillege, M.A. Hlatky, W. Hoffmann, P. Hoffmann, O. Holmen, J.J. Houwing-Duistermaat, T. Illig, A. Isaacs, A.L. James, J. Jeff, B. Johansen, Å. Johansson, J. Jolley, T. Juliusdottir, J. Junttila, A.N. Kho, L. Kinnunen, N. Klopp, T. Kocher, W. Kratzer, P. Lichtner, L. Lind, J. Lindström, S. Lobbens, M. Lorentzon, Y. Lu, V. Lyssenko, P.K.E. Magnusson, A. Mahajan, M. Maillard, W.L. McArdle, C.A. McKenzie, S. McLachlan, P.J. McLaren, C. Menni, S. Merger, L. Milani, A. Moayyeri, K.L. Monda, M.A. Morken, G. Müller, M. Müller-Nurasyid, A.W. Musk, N. Narisu, M. Nauck, I.M. Nolte, M.M. Nöthen, L. Oozageer, S. Pilz, N.W. Rayner, F. Renstrom, N.R. Robertson, L.M. Rose, R. Roussel, S. Sanna, H. Scharnagl, S. Scholtens, F.R. Schumacher, H. Schunkert, R.A. Scott, J. Sehmi, T. Seufferlein, J. Shi, K. Silventoinen, J.H. Smit, A.V. Smith, J. Smolonska, A. V. Stanton, K. Stirrups, D.J. Stott, H.M. Stringham, J. Sundström, M.A. Swertz, A.-C. Syvänen, B.O. Tayo, G. Thorleifsson, J.P. Tyrer, S. van Dijk, N.M. van Schoor, N. van der Velde, D. van Heemst, F.V.A. van Oort, S.H. Vermeulen, N. Verweij, J. M. Vonk, L.L. Waite, M. Waldenberger, R. Wennauer, L.R. Wilkens, C. Willenborg, T. Wilsgaard, M.K. Wojczynski, A. Wong, A.F. Wright, Q. Zhang, D. Arveiler, S.J. L. Bakker, J. Beilby, R.N. Bergman, S. Bergmann, R. Biffar, J. Blangero, D. I. Boomsma, S.R. Bornstein, P. Bovet, P. Brambilla, M.J. Brown, H. Campbell, M. J. Caulfield, A. Chakravarti, R. Collins, F.S. Collins, D.C. Crawford, L.A. Cupples, J. Danesh, U. de Faire, H.M. den Ruijter, R. Erbel, J. Erdmann, J.G. Eriksson, M. Farrall, E. Ferrannini, J. Ferrières, I. Ford, N.G. Forouhi, T. Forrester, R. T. Gansevoort, P.V. Gejman, C. Gieger, A. Golay, O. Gottesman, V. Gudnason, U. Gyllensten, D.W. Haas, A.S. Hall, T.B. Harris, A.T. Hattersley, A.C. Heath, C. Hengstenberg, A.A. Hicks, L.A. Hindorff, A.D. Hingorani, A. Hofman, G. K. Hovingh, S.E. Humphries, S.C. Hunt, E. Hypponen, K.B. Jacobs, M.-R. Jarvelin, P. Jousilahti, A.M. Jula, J. Kaprio, J.J.P. Kastelein, M. Kayser, F. Kee, S. M. Keinanen-Kiukaanniemi, L.A. Kiemeney, J.S. Kooner, C. Kooperberg, S. Koskinen, P. Kovacs, A.T. Kraja, M. Kumari, J. Kuusisto, T.A. Lakka, C. Langenberg, L. Le Marchand, T. Lehtimäki, S. Lupoli, P.A.F. Madden, S. Männistö, P. Manunta, A. Marette, T.C. Matise, B. McKnight, T. Meitinger, F. L. Moll, G.W. Montgomery, A.D. Morris, A.P. Morris, J.C. Murray, M. Nelis, C. Ohlsson, A.J. Oldehinkel, K.K. Ong, W.H. Ouwehand, G. Pasterkamp, A. Peters, P.P. Pramstaller, J.F. Price, L. Qi, O.T. Raitakari, T. Rankinen, D.C. Rao, T.K. Rice, M. Ritchie, I. Rudan, V. Salomaa, N.J. Samani, J. Saramies, M.A. Sarzynski, P.E. H. Schwarz, S. Sebert, P. Sever, A.R. Shuldiner, J. Sinisalo, V. Steinthorsdottir, R. P. Stolk, J.-C. Tardif, A. Tönjes, A. Tremblay, E. Tremoli, J. Virtamo, M.-C. Vohl, P. Amouyel, F.W. Asselbergs, T.L. Assimes, M. Bochud, B.O. Boehm, E. Boerwinkle, E.P. Bottinger, C. Bouchard, S. Cauchi, J.C. Chambers, S.J. Chanock, R.S. Cooper, P.I.W. de Bakker, G. Dedoussis, L. Ferrucci, P.W. Franks, P. Froguel, L.C. Groop, C. A. Haiman, A. Hamsten, M.G. Hayes, J. Hui, D.J. Hunter, K. Hveem, J.W. Jukema, R.C. Kaplan, M. Kivimaki, D. Kuh, M. Laakso, Y. Liu, N.G. Martin, W. März, M. Melbye, S. Moebus, P.B. Munroe, I. Njølstad, B.A. Oostra, C.N.A. Palmer, N. L. Pedersen, M. Perola, L. Pérusse, U. Peters, J.E. Powell, C. Power, T. Quertermous, R. Rauramaa, E. Reinmaa, P.M. Ridker, F. Rivadeneira, J.I. Rotter, T.E. Saaristo, D. Saleheen, D. Schlessinger, P.E. Slagboom, H. Snieder, T.D. Spector, K. Strauch, M. Stumvoll, J. Tuomilehto, M. Uusitupa, P. van der Harst, H. Völzke, M. Walker, N.J. Wareham, H. Watkins, H.-E. Wichmann, J.F. Wilson, P. Zanen, P. Deloukas, I.M. Heid, C.M. Lindgren, K.L. Mohlke, E.K. Speliotes, U. Thorsteinsdottir, I. Barroso, C.S. Fox, K.E. North, D.P. Strachan, J.S. Beckmann, S.I. Berndt, M. Boehnke, I.B. Borecki, M.I. McCarthy, A. Metspalu, K. Stefansson, A. G. Uitterlinden, C.M. van Duijn, L. Franke, C.J. Willer, A.L. Price, G. Lettre, R.J. F. Loos, M.N. Weedon, E. Ingelsson, J.R. O'Connell, G.R. Abecasis, D.I. Chasman, M.E. Goddard, P.M. Visscher, J.N. Hirschhorn, T.M. Frayling, Defining the role of common variation in the genomic and biological architecture of adult human height, Nat. Genet. 46 (2014) 1173–1186, https://doi.org/10.1038/ng.3097.

[20] S.I. Berndt, S. Gustafsson, R. Mägi, A. Ganna, E. Wheeler, M.F. Feitosa, A.E. Justice, K.L. Monda, D.C. Croteau-Chonka, F.R. Day, T. Esko, T. Fall, T. Ferreira, D. Gentilini, A.U. Jackson, J. Luan, J.C. Randall, S. Vedantam, C.J. Willer, T. W. Winkler, A.R. Wood, T. Workalemahu, Y.-J. Hu, S.H. Lee, L. Liang, D.-Y. Lin, J. L. Min, B.M. Neale, G. Thorleifsson, J. Yang, E. Albrecht, N. Amin, J.L. Bragg-Gresham, G. Cadby, M. den Heijer, N. Eklund, K. Fischer, A. Goel, J.-J. Hottenga, J. E. Huffman, I. Jarick, Å. Johansson, T. Johnson, S. Kanoni, M.E. Kleber, I.R. König, K. Kristiansson, Z. Kutalik, C. Lamina, C. Lecoeur, G. Li, M. Mangino, W. L. McArdle, C. Medina-Gomez, M. Müller-Nurasyid, J.S. Ngwa, I.M. Nolte, L. Paternoster, S. Pechlivanis, M. Perola, M.J. Peters, M. Preuss, L.M. Rose, J. Shi, D. Shungin, A.V. Smith, R.J. Strawbridge, I. Surakka, A. Teumer, M.D. Trip, J. Tyrer, J.V. Van Vliet-Ostaptchouk, L. Vandenput, L.L. Waite, J.H. Zhao, D. Absher, F.W. Asselbergs, M. Atalay, A.P. Attwood, A.J. Balmforth, H. Basart, J. Beilby, L.L. Bonnycastle, P. Brambilla, M. Bruinenberg, H. Campbell, D. I. Chasman, P.S. Chines, F.S. Collins, J.M. Connell, W.O. Cookson, U. de Faire, F. de Vegt, M. Dei, M. Dimitriou, S. Edkins, K. Estrada, D.M. Evans, M. Farrall, M. M. Ferrario, J. Ferrières, L. Franke, F. Frau, P.V. Gejman, H. Grallert, H. Grönberg, V. Gudnason, A.S. Hall, P. Hall, A.-L. Hartikainen, C. Hayward, N.L. Heard-Costa, A.C. Heath, J. Hebebrand, G. Homuth, F.B. Hu, S.E. Hunt, E. Hyppönen, C. Iribarren, K.B. Jacobs, J.-O. Jansson, A. Jula, M. Kähönen, S. Kathiresan, F. Kee, K.-T. Khaw, M. Kivimäki, W. Koenig, A.T. Kraja, M. Kumari, K. Kuulasmaa, J. Kuusisto, J.H. Laitinen, T.A. Lakka, C. Langenberg, L.J. Launer, L. Lind, J. Lindström, J. Liu, A. Liuzzi, M.-L. Lokki, M. Lorentzon, P.A. Madden, P. K. Magnusson, P. Manunta, D. Marek, W. März, I.M. Leach, B. McKnight, S. E. Medland, E. Mihailov, L. Milani, G.W. Montgomery, V. Mooser, T.W. Mühleisen, P.B. Munroe, A.W. Musk, N. Narisu, G. Navis, G. Nicholson, E.A. Nohr, K.K. Ong, B. A. Oostra, C.N.A. Palmer, A. Palotie, J.F. Peden, N. Pedersen, A. Peters, O. Polasek, A. Pouta, P.P. Pramstaller, I. Prokopenko, C. Pütter, A. Radhakrishnan, O. Raitakari, A. Rendon, F. Rivadeneira, I. Rudan, T.E. Saaristo, J.G. Sambrook, A. R. Sanders, S. Sanna, J. Saramies, S. Schipf, S. Schreiber, H. Schunkert, S.-Y. Shin, S. Signorini, J. Sinisalo, B. Skrobek, N. Soranzo, A. Stančáková, K. Stark, J. C. Stephens, K. Stirrups, R.P. Stolk, M. Stumvoll, A.J. Swift, E.V. Theodoraki, B. Thorand, D.-A. Tregouet, E. Tremoli, M.M. Van der Klauw, J.B.J. van Meurs, S. H. Vermeulen, J. Viikari, J. Virtamo, V. Vitart, G. Waeber, Z. Wang, E. Widén, S. H. Wild, G. Willemsen, B.R. Winkelmann, J.C.M. Witteman, B.H.R. Wolffenbuttel, A. Wong, A.F. Wright, M.C. Zillikens, P. Amouyel, B.O. Boehm, E. Boerwinkle, D. I. Boomsma, M.J. Caulfield, S.J. Chanock, L.A. Cupples, D. Cusi, G.V. Dedoussis, J. Erdmann, J.G. Eriksson, P.W. Franks, P. Froguel, C. Gieger, U. Gyllensten, A. Hamsten, T.B. Harris, C. Hengstenberg, A.A. Hicks, A. Hingorani, A. Hinney,

A. Hofman, K.G. Hovingh, K. Hveem, T. Illig, M.-R. Jarvelin, K.-H. Jöckel, S. M. Keinanen-Kiukaanniemi, L.A. Kiemeney, D. Kuh, M. Laakso, T. Lehtimäki, D. F. Levinson, N.G. Martin, A. Metspalu, A.D. Morris, M.S. Nieminen, I. Njølstad, C. Ohlsson, A.J. Oldehinkel, W.H. Ouwehand, L.J. Palmer, B. Penninx, C. Power, M.A. Province, B.M. Psaty, L. Qi, R. Rauramaa, P.M. Ridker, S. Ripatti, V. Salomaa, N.J. Samani, H. Snieder, T.I.A. Sørensen, T.D. Spector, K. Stefansson, A. Tönjes, J. Tuomilehto, A.G. Uitterlinden, M. Uusitupa, P. van der Harst, P. Vollenweider, H. Wallaschofski, N.J. Wareham, H. Watkins, H.-E. Wichmann, J.F. Wilson, G. R. Abecasis, T.L. Assimes, I. Barroso, M. Boehnke, I.B. Borecki, P. Deloukas, C. S. Fox, T. Frayling, L.C. Groop, T. Haritunian, I.M. Heid, D. Hunter, R.C. Kaplan, F. Karpe, M.F. Moffatt, K.L. Mohlke, J.R. O'Connell, Y. Pawitan, E.E. Schadt, D. Schlessinger, V. Steinthorsdottir, D.P. Strachan, U. Thorsteinsdottir, C.M. van Duijn, P.M. Visscher, A.M. Di Blasio, J.N. Hirschhorn, C.M. Lindgren, A.P. Morris, D. Meyre, A. Scherag, M.I. McCarthy, E.K. Speliotes, K.E. North, R.J.F. Loos, E. Ingelsson, Genome-wide meta-analysis identifies 11 new loci for anthropometric traits and provides insights into genetic architecture, Nat. Genet. 45 (2013) 501–512, https://doi.org/10.1038/ng.2606.

[21] S.S. Nishizaki, A.P. Boyle, Mining the unknown: assigning function to noncoding single nucleotide polymorphisms, Trends Genet. 33 (2017) 34–45, https://doi.org/10.1016/j.tig.2016.10.008.

[22] E. Cano-Gamez, G. Trynka, From GWAS to function: using functional genomics to identify the mechanisms underlying complex diseases, Front. Genet. 11 (2020) 424, https://doi.org/10.3389/fgene.2020.00424.

[23] L. Hou, H. Zhao, A review of post-GWAS prioritization approaches, Front. Genet. 4 (2013) 280, https://doi.org/10.3389/fgene.2013.00280.

[24] R.D. Cox, C.D. Church, Mouse models and the interpretation of human GWAS in type 2 diabetes and obesity, Dis. Model. Mech. 4 (2011) 155–164, https://doi.org/10.1242/dmm.000414.

[25] H.-J. Chung, J. Liu, M. Dundr, Z. Nie, S. Sanford, D. Levens, FBPs are calibrated molecular tools to adjust gene expression, Mol. Cell. Biol. 26 (2006) 6584–6597, https://doi.org/10.1128/MCB.00754-06.

[26] J. Liu, F. Kouzine, Z. Nie, H.-J. Chung, Z. Elisha-Feil, A. Weber, K. Zhao, D. Levens, The FUSE/FBP/FIR/TFIIH system is a molecular machine programming a pulse of c-myc expression, EMBO J. 25 (2006) 2119–2130, https://doi.org/10.1038/sj.emboj.7601101.

[27] J. Duan, X. Bao, X. Ma, Y. Zhang, D. Ni, H. Wang, F. Zhang, Q. Du, Y. Fan, J. Chen, S. Wu, X. Li, Y. Gao, X. Zhang, Upregulation of far upstream element-binding protein 1 (FUBP1) promotes tumor proliferation and tumorigenesis of clear cell renal cell carcinoma, PLoS One 12 (2017) e0169852, https://doi.org/10.1371/journal.pone.0169852.

[28] L. Yang, J. Zhu, J. Zhang, B. Bao, C. Guan, X. Yang, Y. Liu, Y. Huang, R. Ni, L. Ji, Far upstream element-binding protein 1 (FUBP1) is a potential c-Myc regulator in esophageal squamous cell carcinoma (ESCC) and its expression promotes ESCC progression, Tumour Biol. 37 (2016) 4115–4126, https://doi.org/10.1007/s13277-015-4263-8.

[29] C. Bettegowda, N. Agrawal, Y. Jiao, M. Sausen, L.D. Wood, R.H. Hruban, F. J. Rodriguez, D.P. Cahill, R. McLendon, G. Riggins, V.E. Velculescu, S.M. Oba-Shinjo, S.K.N. Marie, B. Vogelstein, D. Bigner, H. Yan, N. Papadopoulos, K. W. Kinzler, Mutations in CIC and FUBP1 contribute to human oligodendroglioma, Science (80) 333 (2011) 1453–1455, https://doi.org/10.1126/science.1210557.

[30] W. Zhou, Y.J. Chung, E.R. Parrilla Castellar, Y. Zheng, H.-J. Chung, R. Bandle, J. Liu, L. Tessarollo, E. Batchelor, P.D. Aplan, D. Levens, Far upstream element binding protein plays a crucial role in embryonic development, hematopoiesis, and stabilizing Myc expression levels, Am. J. Pathol. 186 (2016) 701–715, https://doi.org/10.1016/j.ajpath.2015.10.028.

[31] R. Gherzi, K.-Y. Lee, P. Briata, D. Wegmüller, C. Moroni, M. Karin, C.-Y. Chen, A KH domain RNA binding protein, KSRP, promotes ARE-directed mRNA turnover by recruiting the degradation machinery, Mol. Cell 14 (2004) 571–583, https://doi.org/10.1016/j.molcel.2004.05.002.

[32] H. Min, C.W. Turck, J.M. Nikolic, D.L. Black, A new regulatory protein, KSRP, mediates exon inclusion through an intronic splicing enhancer, Genes Dev. 11 (1997) 1023–1036.

[33] R. Winzen, B.K. Thakur, O. Dittrich-Breiholz, M. Shah, N. Redich, S. Dhamija, M. Kracht, H. Holtmann, Functional analysis of KSRP interaction with the AU-rich element of Interleukin-8 and identification of inflammatory mRNA targets, Mol. Cell. Biol. 27 (2007) 8388–8400, https://doi.org/10.1128/MCB.01493-07.

[34] M. Pasero, M. Giovarelli, G. Bucci, R. Gherzi, P. Briata, Bone morphogenetic protein/SMAD signaling orients cell fate decision by impairing KSRP-dependent microRNA maturation, Cell Rep. 2 (2012) 1159–1168, https://doi.org/10.1016/j.celrep.2012.10.020.

[35] D. Pruksakorn, P. Teeyakasem, J. Klangjorhor, P. Chaiyawat, J. Settakorn, P. Diskul-Na-Ayudthaya, D. Chokchaichamnankit, P. Pothacharoen, C. Srisomsap, Overexpression of KH-type splicing regulatory protein regulates proliferation, migration, and implantation ability of osteosarcoma, Int. J. Oncol. 49 (2016) 903–912, https://doi.org/10.3892/ijo.2016.3601.

[36] Z.Q. Zhou, C.Y. Shung, S. Ota, H. Akiyama, D.R. Keene, P.J. Hurlin, Sequential and coordinated actions of c-Myc and N-Myc control appendicular skeletal development, PLoS One 6 (2011) e18795, https://doi.org/10.1371/journal.pone.0018795.

[37] M. Iwamoto, K. Yagami, P. Lu Valle, B.R. Olsen, C.J. Petropoulos, D.L. Ewert, M. Pacifici, Expression and role of c-myc in chondrocytes undergoing endochondral ossification, J. Biol. Chem. 268 (1993) 9645–9652.

[38] J.W. Hofmann, X. Zhao, M. De Cecco, A.L. Peterson, L. Pagliaroli, J. Manivannan, G.B. Hubbard, Y. Ikeno, Y. Zhang, B. Feng, X. Li, T. Serre, W. Qi, H. Van Remmen, R.A. Miller, K.G. Bath, R. de Cabo, H. Xu, N. Neretti, J.M. Sedivy, Reduced expression of MYC increases longevity and enhances healthspan, Cell 160 (2015) 477–488, https://doi.org/10.1016/j.cell.2014.12.016.

[39] GTEx Consortium, The GTEx Consortium atlas of genetic regulatory effects across human tissues, Science 369 (2020) 1318–1330, https://doi.org/10.1126/science.aaz1776.

[40] B.-H. Gau, T.-M. Chen, Y.-H.J. Shih, H.S. Sun, FUBP3 interacts with FGF9 3′ microsatellite and positively regulates FGF9 translation, Nucleic Acids Res. 39 (2011) 3582–3593, https://doi.org/10.1093/nar/gkq1295.

[41] M. Rodriguez-Zabala, M. Aza-Carmona, C.I. Rivera-Pedroza, A. Belinchón, I. Guerrero-Zapata, J. Barraza-García, E. Vallespin, M. Lu, A. del Pozo, M. J. Glucksman, F. Santos-Simarro, K.E. Heath, FGF9 mutation causes craniosynostosis along with multiple synostoses, Hum. Mutat. 38 (2017) 1471–1476, https://doi.org/10.1002/humu.23292.

[42] I.H. Hung, G.C. Schoenwolf, M. Lewandoski, D.M. Ornitz, A combined series of Fgf9 and Fgf18 mutant alleles identifies unique and redundant roles in skeletal development, Dev. Biol. 411 (2016) 72–84, https://doi.org/10.1016/j.ydbio.2016.01.008.

[43] X. Wu, M. Gu, L. Huang, X. Liu, H. Zhang, X. Ding, J. Xu, B. Cui, L. Wang, S. Lu, X. Chen, H. Zhang, W. Huang, W. Yuan, J. Yang, Q. Gu, J. Fei, Z. Chen, Z. Yuan, Z. Wang, Multiple synostoses syndrome is due to a missense mutation in exon 2 of FGF9 gene, Am. J. Hum. Genet. 85 (2009) 53–63, https://doi.org/10.1016/j.ajhg.2009.06.007.

[44] I.H. Hung, K. Yu, K.J. Lavine, D.M. Ornitz, FGF9 regulates early hypertrophic chondrocyte differentiation and skeletal vascularization in the developing stylopod, Dev. Biol. 307 (2007) 300–313, https://doi.org/10.1016/j.ydbio.2007.04.048.

[45] R. Brommage, C. Ohlsson, High fidelity of mouse models mimicking human genetic skeletal disorders, Front. Endocrinol. (Lausanne). 10 (2020), https://doi.org/10.3389/fendo.2019.00934.

[46] R.J. Pruim, R.P. Welch, S. Sanna, T.M. Teslovich, P.S. Chines, T.P. Gliedt, M. Boehnke, G.R. Abecasis, C.J. Willer, LocusZoom: regional visualization of genome-wide association scan results, Bioinformatics 26 (2010) 2336–2337, https://doi.org/10.1093/bioinformatics/btq419.

[47] W.C. Skarnes, B. Rosen, A.P. West, M. Koutsourakis, W. Bushell, V. Iyer, A. O. Mujica, M. Thomas, J. Harrow, T. Cox, D. Jackson, J. Severin, P. Biggs, J. Fu, M. Nefedov, P.J. de Jong, A.F. Stewart, A. Bradley, A conditional knockout resource for the genome-wide study of mouse gene function, Nature 474 (2011) 337–342, https://doi.org/10.1038/nature10163.

[48] V.R. Souza, E. Mendes, M. Casaro, A.T.F.B. Antiorio, F.A. Oliveira, C.M. Ferreira, Description of ovariectomy protocol in mice, in: P.C. Guest (Ed.), Pre-Clinical Model. Tech. Protoc, Springer, New York, New York, NY, 2019, pp. 303–309, https://doi.org/10.1007/978-1-4939-8994-2_29.

[49] N.C. Butterfield, J.G. Logan, J. Waung, G.R. Williams, J.H.D. Bassett, Quantitative X-ray imaging of mouse bone by faxitron, in: A.I. Idris (Ed.), Bone Res. Protoc, Springer, New York, New York, NY, 2019, pp. 559–569, https://doi.org/10.1007/978-1-4939-8997-3_30.

[50] E. Demidenko, Kolmogorov-Smirnov test for image comparison, in: A. Lagana, M. L. Gavrilova, V. Kumar, Y. Mun, C.J.K. Tan, O. Gervasi (Eds.), Lect. Notes Comput. Sci, Springer, Berlin, Heidelberg, 2004, pp. 933–939, https://doi.org/10.1007/978-3-540-24768-5_100.

[51] R.J. Van 't Hof, E. Dall'Ara, Analysis of bone architecture in rodents using micro-computed tomography, Methods Mol. Biol. 1914 (2019) 507–531, https://doi.org/10.1007/978-1-4939-8997-3_28.

[52] J.H.D. Bassett, A. Boyde, P.G.T. Howell, R.H. Bassett, T.M. Galliford, M. Archanco, H. Evans, M.A. Lawson, P. Croucher, D.L. St, V.A. Germain, G.R. Williams Galton, Optimal bone strength and mineralization requires the type 2 iodothyronine deiodinase in osteoblasts, Proc. Natl. Acad. Sci. 107 (2010) 7604–7609, https://doi.org/10.1073/pnas.0911346107.

[53] J.H.D. Bassett, A. van der Spek, J.G. Logan, A. Gogakos, J. Bagchi-Chakraborty, A. J. Williams, E. Murphy, C. van Zeijl, J. Down, P.I. Croucher, A. Boyde, A. Boelen, G. R. Williams, Thyrostimulin regulates osteoblastic bone formation during early skeletal development, Endocrinology 156 (2015) 3098–3113, https://doi.org/10.1210/en.2014-1943.

[54] D.W. Dempster, J.E. Compston, M.K. Drezner, F.H. Glorieux, J.A. Kanis, H. Malluche, P.J. Meunier, S.M. Ott, R.R. Recker, A.M. Parfitt, Standardized nomenclature, symbols, and units for bone histomorphometry: a 2012 update of the report of the ASBMR Histomorphometry Nomenclature Committee, J. Bone Miner. Res. 28 (2013) 2–17, https://doi.org/10.1002/jbmr.1805.

[55] R.J. Van 't Hof, L. Rose, E. Bassonga, A. Daroszewska, Open source software for semi-automated histomorphometry of bone resorption and formation parameters, Bone 99 (2017) 69–79, https://doi.org/10.1016/j.bone.2017.03.051.

[56] L. Yengo, J. Sidorenko, K.E. Kemper, Z. Zheng, A.R. Wood, M.N. Weedon, T. M. Frayling, J. Hirschhorn, J. Yang, P.M. Visscher, GIANT Consortium, Meta-analysis of genome-wide association studies for height and body mass index in ~700000 individuals of European ancestry, Hum. Mol. Genet. 27 (2018) 3641–3649, https://doi.org/10.1093/hmg/ddy271.

[57] D.L. Nicolae, E. Gamazon, W. Zhang, S. Duan, M.E. Dolan, N.J. Cox, Trait-associated SNPs are more likely to be eQTLs: annotation to enhance discovery from GWAS, PLoS Genet. 6 (2010) e1000888, https://doi.org/10.1371/journal.pgen.1000888.

[58] A.L. Swan, C. Schütt, J. Rozman, M. Del Mar Muñiz, S. Moreno, M. Brandmaier, S. Simon, M. Leuchtenberger, R. Griffiths, P. Brommage, H. Keskivali-Bond, T. Grallert, R. Werner, L. Teperino, G. Becker, A. Miller, J.R. Moshiri, D.D. Seavitt, T.F. Cissell, E.F. Meehan, C.J. Acar, A.M. Lelliott, M.-F. Flenniken, T. Champy, A. Sorg, R.E. Ayadi, H. Braun, M.E. Cater, P. Dickinson, J. Flicek, E.J. Gallegos, J. D. Ghirardello, S. Heaney, C. Jacquot, J.G. Lally, L. Logan, J. Teboul, N. Mason,

C. Spielmann, S.A. McKerlie, L.M.J. Murray, K.F. Nutter, H. Odfalk, J. Parkinson, C. L. Prochazka, M. Reynolds, F. Selloum, K.L. Spoutil, T.S. Svenson, S.E. Vales, J. K. Wells, R. White, W. Sedlacek, K.C.K. Wurst, P.I. Lloyd, H. Croucher, G.R. Fuchs, J.H.D. Williams, V. Bassett, Y. Gailus-Durner, A.-M. Herault, S.D.M. Mallon, P. Brown, M. Mayer-Kuckuk, Hrabe de Angelis, IMPC Consortium, Mouse mutant phenotyping at scale reveals novel genes controlling bone mineral density, PLoS Genet. 16 (2020) e1009190, https://doi.org/10.1371/journal.pgen.1009190.

[59] Z. Li, J.A. Votava, G.J.M. Zajac, J.N. Nguyen, F.B. Leyva Jaimes, S.M. Ly, J. A. Brinkman, M. De Giorgi, S. Kaul, C.L. Green, S.L. St Clair, S.L. Belisle, J.M. Rios, D.W. Nelson, M.G. Sorci-Thomas, W.R. Lagor, D.W. Lamming, C.-L. Eric Yen, B. W. Parks, Integrating mouse and human genetic data to move beyond GWAS and identify causal genes in cholesterol metabolism, Cell Metab. 31 (2020), https://doi.org/10.1016/j.cmet.2020.02.015, 741-754.e5.

[60] O.T. Hammouda, M.Y. Wu, V. Kaul, J. Gierten, T. Thumberger, J. Wittbrodt, In vivo identification and validation of novel potential predictors for human cardiovascular diseases, PLoS One 16 (2021) e0261572, https://doi.org/10.1371/journal.pone.0261572.

[61] A.J. Alsheikh, S. Wollenhaupt, E.A. King, J. Reeb, S. Ghosh, L.R. Stolzenburg, S. Tamim, J. Lazar, J.W. Davis, H.J. Jacob, The landscape of GWAS validation; systematic review identifying 309 validated non-coding variants across 130 human diseases, BMC Med. Genet. 15 (2022) 74, https://doi.org/10.1186/s12920-022-01216-w.

[62] E. Porcu, S. Rüeger, K. Lepik, F.A. Santoni, A. Reymond, Z. Kutalik, Mendelian randomization integrating GWAS and eQTL data reveals genetic determinants of complex and clinical traits, Nat. Commun. 10 (2019) 3300, https://doi.org/10.1038/s41467-019-10936-0.

[63] M.J. Flister, S.-W. Tsaih, C.C. O'Meara, B. Endres, M.J. Hoffman, A.M. Geurts, M. R. Dwinell, J. Lazar, H.J. Jacob, C. Moreno, Identifying multiple causative genes at a single GWAS locus, Genome Res. 23 (2013) 1996–2002, https://doi.org/10.1101/gr.160283.113.

[64] R. Duncan, L. Bazar, G. Michelotti, T. Tomonaga, H. Krutzsch, M. Avigan, D. Levens, A sequence-specific, single-strand binding protein activates the far upstream element of c-myc and defines a new DNA-binding motif, Genes Dev. 8 (1994) 465–480.

[65] H.-H. Hsiao, A. Nath, C.-Y. Lin, E.J. Folta-Stogniew, E. Rhoades, D.T. Braddock, Quantitative characterization of the interactions among c-myc transcriptional regulators FUSE, FBP, and FIR, Biochemistry 49 (2010) 4620–4634, https://doi.org/10.1021/bi9021445.

[66] S. Ota, Z.-Q. Zhou, D.R. Keene, P. Knoepfler, P.J. Hurlin, Activities of N-Myc in the developing limb link control of skeletal size with digit separation, Development 134 (2007) 1583–1592, https://doi.org/10.1242/dev.000703.

[67] R. Battaglino, D. Kim, J. Fu, B. Vaage, X.-Y. Fu, P. Stashenko, C-myc is required for osteoclast differentiation, J. Bone Miner. Res. 17 (2002) 763–773, https://doi.org/10.1359/jbmr.2002.17.5.763.

[68] C. Farquharson, J.E. Hesketh, N. Loveridge, The proto-oncogene C-myc is involved in cell differentiation as well as cell proliferation: studies on growth plate chondrocytes in situ, J. Cell. Physiol. 152 (1992) 135–144, https://doi.org/10.1002/jcp.1041520118.

[69] Y. Zheng, W. Dubois, C. Benham, E. Batchelor, D. Levens, FUBP1 and FUBP2 enforce distinct epigenetic setpoints for MYC expression in primary single murine cells, Commun. Biol. 3 (2020) 545, https://doi.org/10.1038/s42003-020-01264-x.

[70] W.-J. Lin, X. Zheng, C.-C. Lin, J. Tsao, X. Zhu, J.J. Cody, J.M. Coleman, R. Gherzi, M. Luo, T.M. Townes, J.N. Parker, C.-Y. Chen, Posttranscriptional control of type I interferon genes by KSRP in the innate immune response against viral infection, Mol. Cell. Biol. 31 (2011) 3196–3207, https://doi.org/10.1128/MCB.05073-11.

[71] C.-F. Chou, Y.-Y. Lin, H.-K. Wang, X. Zhu, M. Giovarelli, P. Briata, R. Gherzi, W. T. Garvey, C.-Y. Chen, KSRP ablation enhances brown fat gene program in white adipose tissue through reduced miR-150 expression, Diabetes 63 (2014) 2949–2961, https://doi.org/10.2337/db13-1901.

[72] H. Zheng, V. Forgetta, Y. Hsu, K. Estrada, A. Rosello-Diez, P.J. Leo, C.L. Dahia, K. H. Park-Min, J.H. Tobias, C. Kooperberg, A. Kleinman, U. Styrkarsdottir, C. Liu, C. Uggla, D.S. Evans, C.M. Nielson, K. Walter, U. Pettersson-Kymmer, S. McCarthy, J. Eriksson, T. Kwan, M. Jhamai, K. Trajanoska, Y. Memari, J. Min, J. Huang, P. Danecek, B. Wilmot, R. Li, W. Chou, L.E. Mokry, A. Moayyeri, M. Claussnitzer, C. Cheng, W. Cheung, C. Medina-Gómez, B. Ge, S. Chen, K. Choi, L. Oei, J. Fraser, R. Kraaij, M.A. Hibbs, C.L. Gregson, D. Paquette, A. Hofman, C. Wibom, G. J. Tranah, M. Marshall, B.B. Gardiner, K. Cremin, P. Auer, L. Hsu, S. Ring, J. Y. Tung, G. Thorleifsson, A.W. Enneman, N.M. van Schoor, L.C.P.G.M. de Groot, N. van der Velde, B. Melin, J.P. Kemp, C. Christiansen, A. Sayers, Y. Zhou, S. Calderari, J. van Rooij, C. Carlson, U. Peters, S. Berlivet, J. Dostie, A. G. Uitterlinden, S.R. Williams, C. Farber, D. Grinberg, A.Z. LaCroix, J. Haessler, D. I. Chasman, F. Giulianini, L.M. Rose, P.M. Ridker, J.A. Eisman, T.V. Nguyen, J. R. Center, X. Nogues, N. Garcia-Giralt, L.L. Launer, V. Gudnason, D. Mellstrom, L. Vandenput, N. Amin, C.M. van Duijn, M.K. Karlsson, O. Ljunggren, O. Svensson, G. Hallmans, F. Rousseau, S. Giroux, J. Bussière, P.P. Arp, F. Koromani, R.L. Prince, J.R. Lewis, B.L. Langdahl, A. Pernille Hermann, J.B. Jensen, S. Kaptoge, K. Khaw, J. Reeve, M.M. Formosa, A. Xuereb-Anastasi, K. Åkesson, F.E. McGuigan, G. Garg, J.M. Olmos, M.T. Zarrabeitia, J.A. Riancho, S.H. Ralston, N. Alonso, X. Jiang, D. Goltzman, T. Pastinen, E. Grundberg, D. Gauguier, E.S. Orwoll, D. Karasik, G. Davey-Smith, A.V. Smith, K. Siggeirsdottir, T.B. Harris, M. Carola Zillikens, J.B. J. van Meurs, U. Thorsteinsdottir, M.T. Maurano, N.J. Timpson, N. Soranzo, R. Durbin, S.G. Wilson, E.E. Ntzani, M.A. Brown, K. Stefansson, D.A. Hinds, T. Spector, L. Adrienne Cupples, C. Ohlsson, C.M.T. Greenwood, R.D. Jackson, D. W. Rowe, C.A. Loomis, D.M. Evans, C.L. Ackert-Bicknell, A.L. Joyner, E.L. Duncan, D.P. Kiel, F. Rivadeneira, J.B. Richards, Whole-genome sequencing identifies EN1 as a determinant of bone density and fracture, Nature 526 (2015) 112–117, https://doi.org/10.1038/nature14878.

[73] Y.-F. Pei, W.-Z. Hu, M.-W. Yan, C.-W. Li, L. Liu, X.-L. Yang, R. Hai, X.-Y. Wang, H. Shen, Q. Tian, H.-W. Deng, L. Zhang, Joint study of two genome-wide association meta-analyses identified 20p12.1 and 20q13.33 for bone mineral density, Bone 110 (2018) 378–385, https://doi.org/10.1016/j.bone.2018.02.027.

[74] D.M. Black, N.K. Arden, L. Palermo, J. Pearson, S.R. Cummings, Prevalent vertebral deformities predict hip fractures and new vertebral deformities but not wrist fractures, J. Bone Miner. Res. 14 (1999) 821–828, https://doi.org/10.1359/jbmr.1999.14.5.821.

[75] C. Cooper, E.J. Atkinson, W. MichaelO'Fallon, J.L. Melton, Incidence of clinically diagnosed vertebral fractures: a population-based study in Rochester, Minnesota, 1985-1989, J. Bone Miner. Res. 7 (2009) 221–227, https://doi.org/10.1002/jbmr.5650070214.

[76] T.W. O'Neill, D. Felsenberg, J. Varlow, C. Cooper, J.A. Kanis, A.J. Silman, The prevalence of vertebral deformity in European men and women: the european vertebral osteoporosis study, J. Bone Miner. Res. 11 (2009) 1010–1018, https://doi.org/10.1002/jbmr.5650110719.

[77] H. Chen, X. Zhou, H. Fujita, M. Onozuka, K.-Y. Kubo, Age-related changes in trabecular and cortical bone microstructure, Int. J. Endocrinol. 2013 (2013) 1–9, https://doi.org/10.1155/2013/213234.

[78] G. Osterhoff, E.F. Morgan, S.J. Shefelbine, L. Karim, L.M. McNamara, P. Augat, Bone mechanical properties and changes with osteoporosis, Injury 47 (2016) S11–S20, https://doi.org/10.1016/S0020-1383(16)47003-8.

[79] J. Li, Q. Bao, S. Chen, H. Liu, J. Feng, H. Qin, A. Li, D. Liu, Y. Shen, Y. Zhao, Z. Zong, Different bone remodeling levels of trabecular and cortical bone in response to changes in Wnt/β-catenin signaling in mice, J. Orthop. Res. 35 (2017) 812–819, https://doi.org/10.1002/jor.23339.

[80] S. Unger, C.R. Ferreira, G.R. Mortier, H. Ali, D.R. Bertola, A. Calder, D.H. Cohn, V. Cormier-Daire, K.M. Girisha, C. Hall, D. Krakow, O. Makitie, S. Mundlos, G. Nishimura, S.P. Robertson, R. Savarirayan, D. Sillence, M. Simon, V.R. Sutton, M.L. Warman, A. Superti-Furga, Nosology of genetic skeletal disorders: 2023 revision, Am. J. Med. Genet. A 191 (2023) 1164–1209, https://doi.org/10.1002/ajmg.a.63132.

[81] M.J. Rock, J. Prenen, V.A. Funari, T.L. Funari, B. Merriman, S.F. Nelson, R. S. Lachman, W.R. Wilcox, S. Reyno, R. Quadrelli, A. Vaglio, G. Owsianik, A. Janssens, T. Voets, S. Ikegawa, T. Nagai, D.L. Rimoin, B. Nilius, D.H. Cohn, Gain-of-function mutations in TRPV4 cause autosomal dominant brachyolmia, Nat. Genet. 40 (2008) 999–1003, https://doi.org/10.1038/ng.166.

[82] A. Klibanski, L. Adams-Campbell, T. Bassford, S. Blair, S. Boden, K. Dickersin, D. Gifford, S. Goldring, K. Hruska, S. Johnson, L. McCauley, W. Russell, Osteoporosis prevention, diagnosis and therapy, JAMA 285 (2001) 785–795.

[83] R.L. Jilka, The relevance of mouse models for investigating age-related bone loss in humans, J. Gerontol. Ser. A Biol. Sci. Med. Sci. 68 (2013) 1209–1217, https://doi.org/10.1093/gerona/glt046.

[84] P.M. Chavassieux, M.E. Arlot, P.J. Meunier, Intersample variation in bone histomorphometry: comparison between parameter values measured on two contiguous transiliac bone biopsies, Calcif. Tissue Int. 37 (1985) 345–350, https://doi.org/10.1007/BF02553699.

[85] P. Ballanti, C. Della Rocca, E. Bonucci, S. Milani, V. Lo Cascio, B. Imbimbo, Sensitivity of bone histomorphometry in the diagnosis of metabolic bone diseases, Pathol. Res. Pract. 185 (1989) 786–789, https://doi.org/10.1016/S0344-0338(89)80240-7.

[86] C.D.P. Wright, S. Vedi, N.J. Garrahan, M. Stanton, S.W. Duffy, J.E. Compston, Combined inter-observer and inter-method variation in bone histomorphometry, Bone 13 (1992) 205–208, https://doi.org/10.1016/8756-3282(92)90198-6.